Environmental Science and Pollution Research (2022) 29:15876–15895
https://doi.org/10.1007/s11356-021-16869-w

RESEARCH ARTICLE

Taguchi optimization of geopolymer concrete produced with rice husk ash and ceramic dust

Selçuk Memiş[1] · Mohamed Ahmed Mohamed Bılal[2]

Received: 14 July 2021 / Accepted: 29 September 2021 / Published online: 11 October 2021

Abstract

Metakaolin, fly ash, and mostly granulated blast furnace slag (GBFS) are traditionally used in the production of geopolymer. This study, adding to the knowledge base on geopolymer concretes as an alternative to cement mixtures, explored an experimental approach that investigates the use of ceramic dust (CD) and rice husk ash (RHA) with high SiO content instead of GBFS in the production of geopolymers. For this purpose, instead of GBFS, RHA at proportions of 0, 5%, 10%, and 15% and CD at proportions of 0, 10%, 20%, and 30% were used in the production of geopolymer concrete. In addition, groups were determined with a Taguchi L16 matrix with NaOH (an important material in geopolymer production) at 12, 14, 16, and 18 molality. Varying combinations of flow diameter, density, porosity, and water absorption rate were used, and their performance under high temperatures in terms of compressive strength was evaluated. The use of RHA in geopolymer concretes produced using CD and RHA had a negative effect on the flow and water absorption rates. However, the use of CD had a positive effect, and geopolymer concretes with high density and porosity were obtained. In addition, it was determined that strengths > 70 MPa could only be obtained if 5–20% CD were used at 14–16 molality. The resistance of geopolymer concretes to high temperatures is lower than normal concretes. However, when comparing RHA and CD, it was determined that the use of CD would be more effective on geopolymer materials, and special measures should be taken at temperatures > 450 °C.

Keywords Slag · Rice husk ash · Waste ceramic powder · Geopolymer concrete · Sodium silicate · Sodium hydroxide · Compressive strength · Flexural strength · Taguchi method · Fire resistance

Introduction

Concrete is one of the most widely used building materials in the world (Memis et al. 2017b; Assi et al. 2018). Its binder is Portland cement (PC). Today, PC is the leading binding material used in building materials and especially in concrete production (Habert et al. 2011; Nimwinya et al. 2016; Memis et al. 2017a; Yaprak et al. 2017; Alnkaa et al. 2018). It is estimated that the annual production of this material will increase by about 50% compared to 2017 levels by the end of 2050, and accordingly it will emit approximately about 1 t of CO_2 per ton of PC production (Khalaj et al. 2014; Amran et al. 2021). In addition to its advantages, PC also has disadvantages. One of these is that it causes negative environmental effects due to the use of fossil fuels in its production and the process of limestone separation, and it creates greenhouse gas emissions with CO_2, which constitutes 65% of global greenhouse gases (Habert et al. 2011; Masi et al. 2014; Nimwinya et al. 2016; Zhou et al. 2016; Alnkaa et al. 2018; Kishore and Gupta 2021). Environmental degradation is a problem that should be evaluated on a global scale. At the world summits held in Kyoto in 1997 and Paris in 2015, the necessity of protecting the environment worldwide was emphasized in the decisions taken, and it was declared that the prevention of disasters depends on the condition that CO_2 emissions should not be > 21%. It was stated that countries with emission rates above this should take necessary measures to reduce their CO_2 emissions by 2030. Despite these decisions, the concrete industry produces approximately 12

Responsible Editor: by Philippe Garrigues

✉ Selçuk Memiş
smemis@kastamonu.edu.tr

[1] Department of Civil Enginineering, Kastamonu University, 37150 Kastamonu, Turkey

[2] Department of Materials Science and Engineering, Institute of Science, Kastamonu University, 37150 Kastamonu, Turkey

billion tons of concrete each year globally, using approximately 1.6–1.89 billion tons of PC, and emits a significant amount of CO_2 as a result (Rashad 2013; Suhendro 2014; El-Gamal et al. 2017). Therefore, approximately 5–8% of the total CO_2 emissions worldwide come from cement production in cement factories (Jithendra and Elavenil 2020; Akbar et al. 2021; Albidah 2021).

The International Energy Agency reported that due to the CO_2 gas produced, there will be an average 1.4–5.8 °C increase in global temperatures in the next century, and as a result sea levels will rise (International Energy Agency; Gielen et al. 2007; Alnkaa et al. 2018; Ghafoor et al. 2021). In reducing these effects, it is necessary either to investigate different methods of reducing CO_2 emissions caused by cement production or use an alternative material to cement using a binder with no/less CO_2 emissions (Rashad 2013; Nimwinya et al. 2016). In the production of these binders, it is an important issue to develop new products that require less energy, emit less CO_2, and have similar properties to existing ones. This has revealed the reuse of industrial waste materials, which can increase mechanical properties and strength, such as fly ash (FA), blast furnace slag (BFS), silica fume, and rice husk ash (RHA) (Komnitsas 2011; Villaquirán-Caicedo and de Gutiérrez 2018).

Solid waste landfills continue to collect large amounts of industrial waste, especially urban waste. To reverse this situation, it may be possible to reduce storage capacities and convert solid waste into an alternative source of energy. This will help reduce the use of resources that cannot naturally renew in natural environments, to conserve energy, and solve problems encountered in minimizing the environmental damage caused by waste storage. Many studies have been carried out on the use of solid waste materials in concrete, changing the properties of cement that contribute significantly to global greenhouse gas emissions, and investigating alternative binders (El-Dieb and Kanaan 2018). These studies have shown that one possible solution to the problem is the production of geopolymer concrete with less CO_2 emissions. For example, the amount of CO_2 released by 0.18 t of carbon fuel used in 1 t of geopolymer production is less than the CO_2 released by 1 t of carbon-containing fuel used for PC production. This means that geopolymer concrete produces approximately six times less CO_2 than PC during manufacture. In addition, it can be predicted that environmental impacts are minimized by using the aforementioned waste materials in geopolymer concrete. Geopolymer concrete is an inorganic polymeric compound that has the potential to be used as an alternative to conventional concrete, and constitutes an important element in environmentally sustainable construction. It is generally produced by alkaline activation of industrial alumina silicate-based waste materials, such as FA and granulated BFS (GBFS) (Rajamane et al. 2011; Darsanasiri et al. 2018).

The geopolymer used in the zeolite-like family of metal binders is known to have emerged in 1970, when Davidovits synthesized an inorganic polymeric material through alkali activation of aluminosilicate (Hu et al. 2009; Hwang and Huynh 2015; Nimwinya et al. 2016; Zhou et al. 2016; Kaur et al. 2018; Ameri et al. 2019). Unlike PC, geometries do not form calcium–silicate–hydrate to form the matrix and strength, but use precursor condensation and alumina gels to achieve structural strength. Geopolymers have a three-dimensional aluminosilicate material structure (Yildizay et al. 2014), and are grouped depending on the Si:Al ratio. This material structure can be explained as the arrangement of Al and Si atoms in a tetrahedral structure in the process of polymerization or when Na^+ or K^+ ions used as alkali create equilibrium with Al ions (Komnitsas 2011; Rajamane et al. 2011; Darsanasiri et al. 2018).

Geopolymers have two main components: alkaline solutions and binder materials. The most common alkaline solutions used in geopolymerization are mixtures of sodium hydroxide (NaOH) or potassium hydroxide (KOH) with sodium silicate (Na_2SiO_3) or potassium silicate (K_2SiO_3) (Abbasi et al. 2016; Villaquirán-Caicedo and de Gutiérrez 2018; Ameri et al. 2019; Amran et al. 2021; Ghafoor et al. 2021). Under highly alkaline conditions, when fast and free reactive silicate aluminates dissolve tetrahedral units in solution, polymerization occurs in the presence of an alkaline hydroxide solution and thus silicate. The strength of geopolymers is also due to the interconnectedness of these structures (Komnitsas 2011). Also, such materials as alumina silicate–based Si- and Al-rich FA, silica fume, GBFS, and red mud can be counted as binding materials (Komnitsas 2011; Rajamane et al. 2011; Khalaj et al. 2014; Sanjayan et al. 2015; Darsanasiri et al. 2018).

Many researchers are working toward attaining a sustainable material and effective management of waste by adding various types of industrial or agricultural waste to concrete. Most studies have focused on industrial products, such as GBFS, steel slag, cement raw-meal powder, and FA, as well as agricultural waste products, such as RHA and palm oil ash, instead of cement or aggregates (Villaquirán-Caicedo and de Gutiérrez 2018; Zareei et al. 2019). In addition, researchers have investigated the effects of using these wastes in geopolymer concrete, one of the alternative materials. Such materials as glass waste (Dadsetan et al. 2021), kaolinitic clays (Heath et al. 2014; Vald et al. 2021), metakaolin (Perera et al. 2006; Kamseu et al. 2010; Zhu et al. 2018; Zawrah et al. 2020; Sarkar and Dana 2021), FA (Assi et al. 2018; Kumar et al. 2019; Yaprak et al. 2019; Zhao et al. 2019; Charkhtab et al. 2021), and BFS (Bernal et al. 2011; Abdel-ghani et al. 2018; Memis et al. 2018; Mayhoub et al. 2020; Yasaswini and Rao 2020), featured prominently in these studies — wherein sustainability analysis was also conducted to evaluate the energy consumption and CO_2

emissions of geopolymer binders — are the most commonly used industrial aluminosilicate materials. In addition, other many studies have shown that agricultural wastes can be used in cementitious materials as ash in concrete, such as RHA (Nuruddin et al. 2014; Hwang and Huynh 2015; Nimwinya et al. 2016; Cannio and Billong 2017; Cristina et al. 2017; Ambedkar et al. 2017; Yaprak et al. 2018b; Darsanasiri et al. 2018), wood waste ash (Cheah and Ramli 2011), cattle manure ash (Şahin et al. 2006; Zhou and Chen 2012; Zhou et al. 2015), corn cob ash (Adesanya and Raheem 2009), palm oil fuel ash (Abdullah, Hussin, Zakaria 2006; Alsubari et al. 2016; Thomas et al. 2017), bamboo stem ash (Rodier et al. 2017), paper mill ash (Corinaldesi et al. 2010), and sugarcane bagasse ash (Ganesan et al. 2007; Sua-Iam and Makul 2013; Deepika et al. 2017; Akbar et al. 2021).

An agricultural waste product, RHA, is a common by-product in rice-producing areas. Much of the husk from rice processing (partly for energy generation) is burned or dumped as waste material. When RHA is used as fuel, it can be burned in biomass-based boilers and power plants. RHA is also a material that can be used as an alternative fuel to meet the energy needs of the ceramic and cement industries. Burning RHA as biofuel causes the waste product called RHA. This ash comprises 22–25% of each unit of RHA burned (Arnold et al. 2017).

The Taguchi method is a statistical technique developed by Genichi Taguchi during the 1950s (Roy 1990). It is a robust statistical method that eliminates unnecessary test by using the orthogonal arrays. The orthogonal array is economical compared to normal experimental design methods, and reduces the number of experiments and minimizes uncontrollable parameters. Taguchi's approach to parameter design provides the design engineer with a systematic and efficient method for determining near-optimum design parameters for performance and cost. The first concept of the Taguchi method is "noise factors," which use the signal:noise (S:N) ratio to analyze this data and predict optimum results. The S/N measures the level of performance and the effect of noise factors on performance and is an evaluation of the stability of performance of an output characteristic (Nuruddin and Bayuji 2009). Target values may be:

For smaller is better, when the goal is to minimize the response, the S:N ratio can be calculated as given in Eq. (1):

$$\frac{S}{N} = -10 \cdot \log_{10}\left(\frac{1}{n}\sum_{i=1}^{n} Y_i^2\right) \tag{1}$$

For larger is better, when the goal is to maximize the response, the S:N ratio is calculated as given in Eq. (2):

$$\frac{S}{N} = -10 \cdot \log_{10}\left(\frac{1}{n}\sum_{i=1}^{n} \frac{1}{Y_i^2}\right) \tag{2}$$

For nominal is better, when the goal is to target the response and it is required to base the S:N ratio on standard deviations only, the S:N ratio is calculated as given in Eq. (3) for the smaller the better:

$$\frac{S}{N} = -10 \cdot \log_{10}\left(\frac{1}{n}\sum_{i=1}^{n} \left(Y_i - Y_0\right)^2\right) \tag{3}$$

Studies on geopolymer concrete using the Taguchi design include Olivia and Nikraz (2012) (the effects of factors and levels on the mechanical and strength properties of geopolymer concrete); Riahi et.al. (2012) (the effect of furnace curing time, temperature, and sodium hydroxide concentration on compressive strength on ash-based geopolymers); Bagheri and Nazari (2014) (compressive strength of fly ash-based geopolymers with reactive granulated blast furnace slag aggregates); Nazari and Sanjayan (2015) (the effects of alumina and silica nanoparticles on water absorption of geopolymers); Siyal et.al (2016) (the effects of parameters on the setting time of fly ash-based geopolymers); Hadi et. al. (2017) (geopolymer concrete design with GGBFS in ambient curing condition); Onoue et. al. (2019) (optimization of the design parameters of fly ash-based geopolymer using); and Jithendra and Elavenil (2020) (the effects of factors and their levels on fluid geopolymer concrete) appear to be used. For the most part, the Taguchi method is used widely in engineering applications, but applications for geopolymer concrete are very limited. Recently, geopolymers have been studied extensively, due to the mechanical, chemical, and physical properties of concrete, possible practical use in the construction industry and sustainable development (Živica et al. 2015). The most important factor in the production of geopolymer concrete is the use of materials with a high reactive Al and Si ratio, and RHA is one that can be used as a source of silica (SiO_2) (ASTM C 136 / C136M-19 2014). The aim of this study was to investigate a cheaper and environmentally friendly material mixture in geopolymer concrete that has less CO_2 emissions and has cementitious properties. The effects of some strength and durability properties in geopolymer concrete using waste ceramic dust (CD; 0, 10%, 20%, and 30%), RHA (0, 5%, 10%, and 15%), and molality 12, 14, 16, and 18 prepared using Taguchi L16 (4^3) design were investigated.

Material and methods

Materials

In the production of geopolymer concrete, mixtures of fine aggregate (ASTM C 136) (ASTM C 136 / C136M-19 2014), with a maximum grain diameter of 4.75 mm traditionally, and silica sand, with a maximum grain diameter of 2 mm, in accordance with TS-EN196-1 were used (TS-EN196-1,

2016). The fineness modulus of aggregates used in the study is 2.14 according to ASTM C 136 and 3.44 for silica sand (ASTM C 136 / C136M-19 2014). Waste ceramic pieces obtained from demolished buildings were used. Ceramic waste was reduced in size manually in the first stage in a laboratory and crushed in a crusher for the small pieces obtained in the second stage. In order for the CD to be used in the mixtures to reach the desired fineness, it was subjected to grinding for 120 min in a mill at a rotation speed of 600 rpm. RHA preparation was carried out under laboratory conditions. The RHA was obtained from the district Tosya of Kastamonu in Turkey. RHA was obtained by an equipment with a combustion chamber in the middle of the husks, which allowed the husks to burn through contact. The fully burned RHA was extracted carefully and the carbon layer avoided as much as possible. The RHA then remained in a ring mill for 60 s to achieve the desired fineness. GBFS was provided by Ereğli Iron and Steel Works Company (Karadeniz Ereğli, Turkey). Chemical compositions of GBFS, CD, and RHA are shown in Table 1. In addition, NaOH and Na_2SiO_3 were preferred as alkali activators in mixtures. NaOH with Na_2SiO_3, which is 97% pure and contains 13% SiO_2 and 30% H_2O, was obtained from the market and used in mixtures.

Mix design

Studies investigating mineral additives in geopolymer concretes were taken into account in forming the groups. In this study, the proportion of CD was 0, 10%, 20%, and 30% (El-Dieb and Kanaan 2018) instead of GBFS, RHA 0, 5%, 10%, and 15% instead of GBFS, and NaOH solution was prepared at 12, 14, 16, and 18 molality (Altoubat et al. 2016). And also, alkaline solution to binder ratio 0.37 was preapared (Shoaei et al. 2019). Variables were determined according to scenarios in which the effects of CD and RHA were able to be determined. In this study, the design of the mixture was determined using the Taguchi L16 matrix (Dave and Bhogayata 2020). Each mix is given a code (Table 2) with a specified letter identifier. In order to determine the effect of each variable in the study, the experimental design should be prepared separately. In this case, the experimental design should be full factorial and as a result 64 different groups should be produced. Partial factorial experimental design was used in the study to save time and material. For this reason, Taguchi optimization technique was applied with Taguchi L16 orthogonal experiment matrix. A total of 16 groups of mixtures were prepared using the Taguchi method (Table 3) using the L16 (4^3) orthogonal array showing all factors and levels.

Table 1 Chemical composition of materials used

Chemical composition (%)	CD	RHA	GBFS
CaO	4.83	0.60	38.27
SiO_2	63.39	96.55	39.94
Al_2O_3	18.42	0.55	14.36
Fe_2O_3	6.54	0.31	1.16
MgO	2.56	0.88	2.74
Na_2O	0.90	1.07	0.52
K_2O	2.91	2.28	0.82
SO_3	0.07	–	0.08

Table 2 Levels considered for each parameter in Taguchi design

Parameters	Code	Level			
		1	2	3	4
CD	C	0%	10%	20%	30%
RHA	R	0%	5%	10%	15%
Molality	M	12	14	16	18

Alkali activator and specimen preparation

Kamseu et al. 2017 and Kaur et al. 2018 stated that that NaOH pellets in 1 L water should be dissolved by adding water in a bottle. In these preparations, after adding NaOH water, it was left for 24 h until it was mixed with the other compound. And also the alkali activator should be prepared by the combination of NaOH and Na_2SiO_3 mixtures.

Table 3 L16 array suggested by Taguchi method for three parameters at four levels

	Mix code	Parameters			
		GBFS (%)	CD (%)	RHA (%)	Molality
1	C0R0M12	100	0	0	12
2	C0R5M14	95	0	5	14
3	C0R10M16	90	0	10	16
4	C0R15M18	85	0	15	18
5	C10R0M14	90	10	0	14
6	C10R5M12	85	10	5	12
7	C10R10M18	80	10	10	18
8	C10R15M16	75	10	15	16
9	C20R0M16	80	20	0	16
10	C20R5M18	75	20	5	18
11	C20R10M12	70	20	10	12
12	C20R15M14	65	20	15	14
13	C30R0M18	70	30	0	18
14	C30R5M16	65	30	5	16
15	C30R10M14	60	30	10	14
16	C30R15M12	55	30	15	12

In this study, the same method was used in the preparation of NaOH solution in mixtures. For this purpose, a certain weight of NaOH was added to this water and the mixture obtained in the corresponding molality. The required amount of NaOH was calculated with the Eq. (40 g (NaOH weight) × molality value = weight of NaOH to be used). The ratio of Na_2SiO_3 to NaOH was fixed as equal (Memis et al. 2018; Yaprak et al. 2018b).

In geopolymer production, mixing sequence and time are very important to ensure the same homogeneity and structure in all mixtures. The amount of materials used in the mixtures according to the Taguchi L16 matrix prepared using mineral:aggregate ratio of 0.60 and the preliminary trial mixes are given in Table 4. The material amounts required were weighed according to the ratios given in Table 4, and the materials entering the mixture were added to a Hobart mixer in three steps (Fig. 1): first dry materials and then alkalis.

The spreading diameter values of the prepared mixtures were determined and the mixtures poured into molds with dimensions of 40 × 40 × 160 mm in accordance with TS EN 196–1 (2016). Finally, the molds are covered with glass plates. Samples were removed from the mold 24 h later and placed in a hot water curing tank at 60° C for 24 h (Omer et al. 2015; Yaprak et al. 2018a; Annakoa et al. 2019; Kaplan et al. 2019; Akbar et al. 2021). Afterwards, the samples were kept under laboratory conditions and in a humid condition, covered with nylon, until the test dates.

Test procedures

Compressive and flexural strength tests were carried out on 40 × 40 × 160 mm samples that had undergone 28-day curing in accordance with BS EN 196–1 (BS EN 196–1 2005). Vertical load application was initiated using a loading cylinder on the upper surface of the prism and loading at a rate of 50 ± 10 N s^{-1} until breakage occurred

Table 4 Amounts of materials used in the gepolymer concrete mix ($kg.m^{-3}$)

Mix code	Na_2SiO_3	NaOH	GBFS	CD	RHA	Sand	Agregate	Water
C0R0M12	150	150	800	0	0	400	800	225
C0R5M14			760		40			
C0R10M16			720		80			
C0R15M18			680		120			
C10R0M14			720	80	0			
C10R5M12			680		40			
C10R10M18			640		80			
C10R15M16			600		120			
C20R0M16			640	160	0			
C20R5M18			600		40			
C20R10M12			560		80			
C20R15M14			455		120			
C30R0M18			560	240	0			
C30R5M16			520		40			
C30R10M14			480		80			
C30R15M12			440		120			

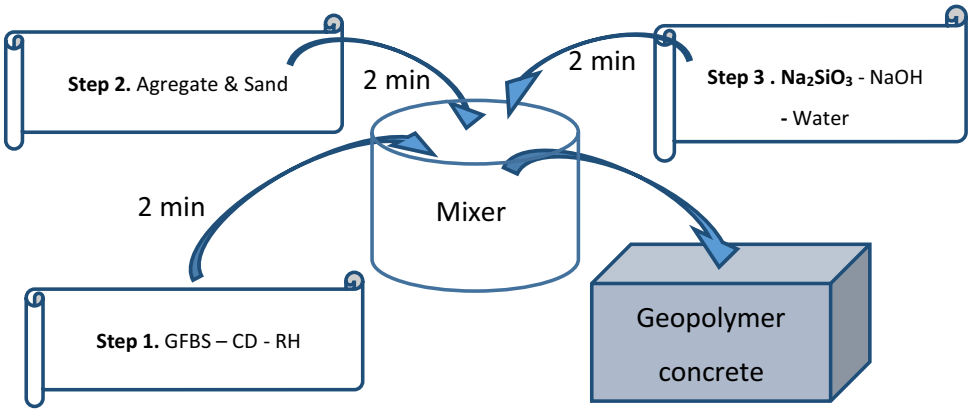

Fig. 1 Mixing process

for flexural strength. Compressive strength tests were performed on two parts obtained from the flexural strength tests. Compressive strength tests were conducted up to 2400 ± 200 N s^{-1} loading speed to each one of the pieces broken in flexural strength. Compressive strength in geopolymer concretes was determined in accordance with TS EN 1015–11 (2020) by determining the load at the moment of breaking. Density and void ratio were determined in accordance with ASTM C642-97 (ASTM C642 1997). This is also useful for developing conversion data for concrete mass and volume, which helps in determining the concrete specifications and revealing differences or variations in different places. Spreading table tests were conducted according to the absence of obstacles in accordance with ASTM C1437 (ASTM C1437-20 2020) and capillary water absorption in accordance with ASTM C1585-04 (2004) has been determined.

Fire resistance tests were made in accordance with ASTM E2748-12a (2017). Within the scope of this study, samples were left at high temperatures of 300 °C, 450 °C, and 600 °C for 1 h (Omer et al. 2015; Tahwia 2017), to determine the effects on the geopolymers at different temperatures. Fire resistance was determined at 28-day samples. Before heating, a drying treatment is usually needed to control explosive spalling (Liang et al. 2018). The samples were exposed to high temperatures up to 300 °C, 450 °C, and 600 °C at a rate of 5 °C/min in a mechanically ventilated electric oven to dry at 105 °C for 24 h (ASTM E831 2014; Omer et al. 2015; Ameri et al. 2019). After the furnace returns to room temperature, strength and weight losses are determined.

Results and discussion

Fresh properties

Flow diameter was measured by filling the cone-shaped mold with the geopolymer mortar and removing the mold after 25 head movements. Flow diameter in the samples (Table 5) was 20–25 cm. With the addition of CD and RHA, the flow diameter tended to increase or decrease depending on the material used. When the change in the flow diameters of the prepared geopolymers was examined statistically (Fig. 2), the use of CD increased the diameter in parallel with the increasing usage rate in the geopolymer mixtures (Fig. 5a). However, when the relationship between RHA and flow diameter was examined (Fig. 2b), the diffusion diameter decreased compared to the statistical averages due to the increasing RHA usage. There was a statistically poor relationship between this decreased RHA and flow diameter. This resulted in a maximum spread diameter of 22 cm only the groups using RHA and stickier mortar in the mixtures using RHA. However, high-flow diameter values, which can be an indicator of good mold settling, showed that CD can be added in addition to the use of RHA in mixtures. Talha et al. explained this as being because alkali activators (NaOH and Na_2SiO_3/NaOH) have higher viscosity than water, and the increased molality of NaOH increases the viscosity of the NaOH solution (Ghafoor et al. 2021). Also, its workability decreased with increasing molality of NaOH, due to the decrease in water content (Görhan and Kürklü 2014; Elyamany et al. 2018). Fine ash particles mixed with viscous alkali activators showed adhesive and cohesive properties.

Table 5 Compressive strength and flexural strenght test results for mixtures

Mix no	Mix code	Slump (mm)	Compressive strength (MPa)				Flexural strength (MPa)			
			3 days	7 days	28 days	90 days	3 days	7 days	28 days	90 days
1	C0R0M12	21	55.40	56.15	60.33	67.61	2.30	2.46	2.48	3.17
2	C0R5M14	22	52.40	57.10	59.42	65.11	1.69	1.83	1.99	2.05
3	C0R10M16	22	46.10	48.30	48.91	50.10	2.61	2.65	2.75	2.96
4	C0R10M18	20	33.50	33.65	34.70	36.68	0.80	0.85	1.19	1.22
5	C10R0M14	21	61.40	65.10	66.74	77.32	2.15	2.19	2.91	3.43
6	C10R5M12	24	62.02	62.45	62.80	64.20	0.14	0.19	0.23	0.38
7	C10R10M18	21	47.41	47.50	49.30	50.20	0.70	0.73	0.82	0.85
8	C10R15M16	22	27.33	27.53	28.62	30.76	0.61	0.76	0.78	0.80
9	C20R0M16	25	63.77	66.97	71.71	78.38	1.15	1.42	2.50	2.57
10	C20R5M18	25	57.92	58.76	62.16	70.96	1.37	1.79	2.17	2.23
11	C20R10M12	25	43.47	44.10	45.21	52.20	2.30	2.37	2.42	2.96
12	C20R15M14	24	25.56	25.73	26.40	27.25	0.58	0.59	0.70	0.69
13	C30R0M18	24	73.70	74.93	77.40	85.31	1.93	2.19	2.61	2.80
14	C30R5M16	25	55.10	55.70	57.90	58.31	0.31	0.43	0.65	0.93
15	C30R10M14	23	33.98	34.21	34.55	35.61	0.31	0.36	0.45	0.71
16	C30R15M12	23	23.88	24.10	24.18	25.46	0.33	0.35	0.38	0.40

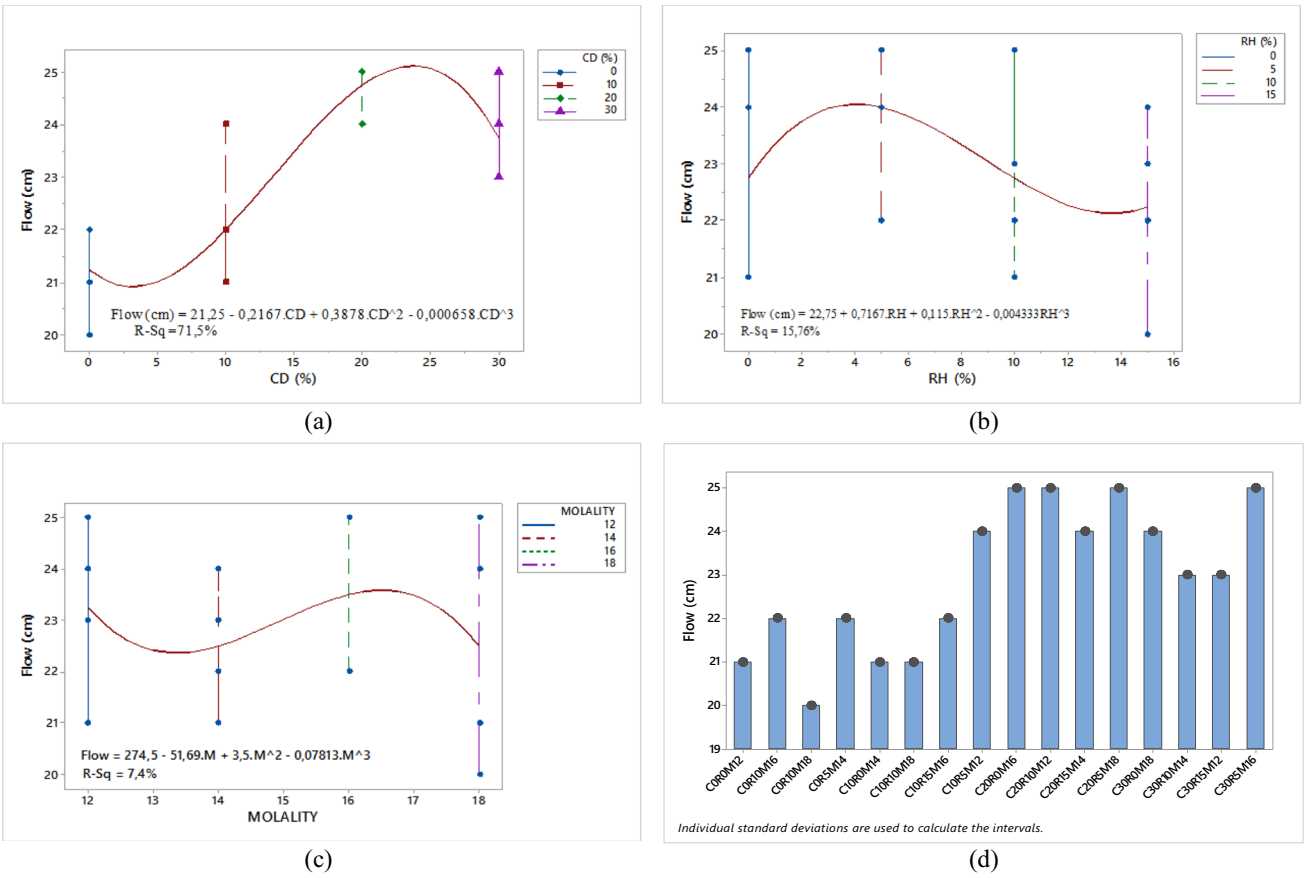

Fig. 2 Relationship between dynamic flow and mineral content

Based on flow diameter (Fig. 3), it was determined that the maximum spreading diameter can be achieved by either using 20–25% CD at 16–18 molality without using RHA or by adding only 5% RHA to this mixture. The minimum flow diameter was possible with the use of 10–15% RHA only at 16–18 molality or with the usage rate not exceeding 5–10% regardless of molality in the use of CD.

Hardened properties

Compressive strengths

Compressive strength values showing the effects of RHA and CD used at different rates depending on varying molality values in geopolymer concretes are given in Table 5. The results reached a final strength of 85 MPa at the end of 90 days at 18 molality with 30% CD used for strength, while the minimum strength was 25.46 MPa in the group where 30% CD and 15% RHA were used at 12 molality. In these groups, when the 90-day final strength values were compared with the 3-day values (Fig. 4), the ratio was 89% in the group with the maximum strength and 94% in the group with the lowest strength. The fact that approximately 90% of the final strengths were reached at 3-day values revealed that the hot water curing selected in this study is an important factor in the compressive strength of geopolymers. In addition, changes in compressive strength according to molality showed a decrease at 12–14 molality compared to increasing CD and RHA, but in the 16–18 molality groups, CD and RHA had a positive effect. This showed that the activators that enter the mixture in groups prepared with low mobility were not sufficient, depending on the powder materials used, and this situation caused a decrease in strength.

When the relationship between the materials used in geopolymers and their compressive strength (Fig. 5) was examined, if only CD were used in the mixtures (Fig. 5a), strength increased according to the increased molality value and the highest strength was reached. However, a decrease in strength was observed due to the negative effect of this change in the ratio of RHA entering and increasing in the mixtures (Fig. 5b). In other words, the use of higher quantities of RHA caused a loss of strength of up to approximately 50%. Molality effect varied due to the materials entering the mixture. In Fig. 5b, strength decreases, with the decrease in usage of GBFS expressing this change in molality (Nath and Sarker 2017). In other words, when making geopolymer

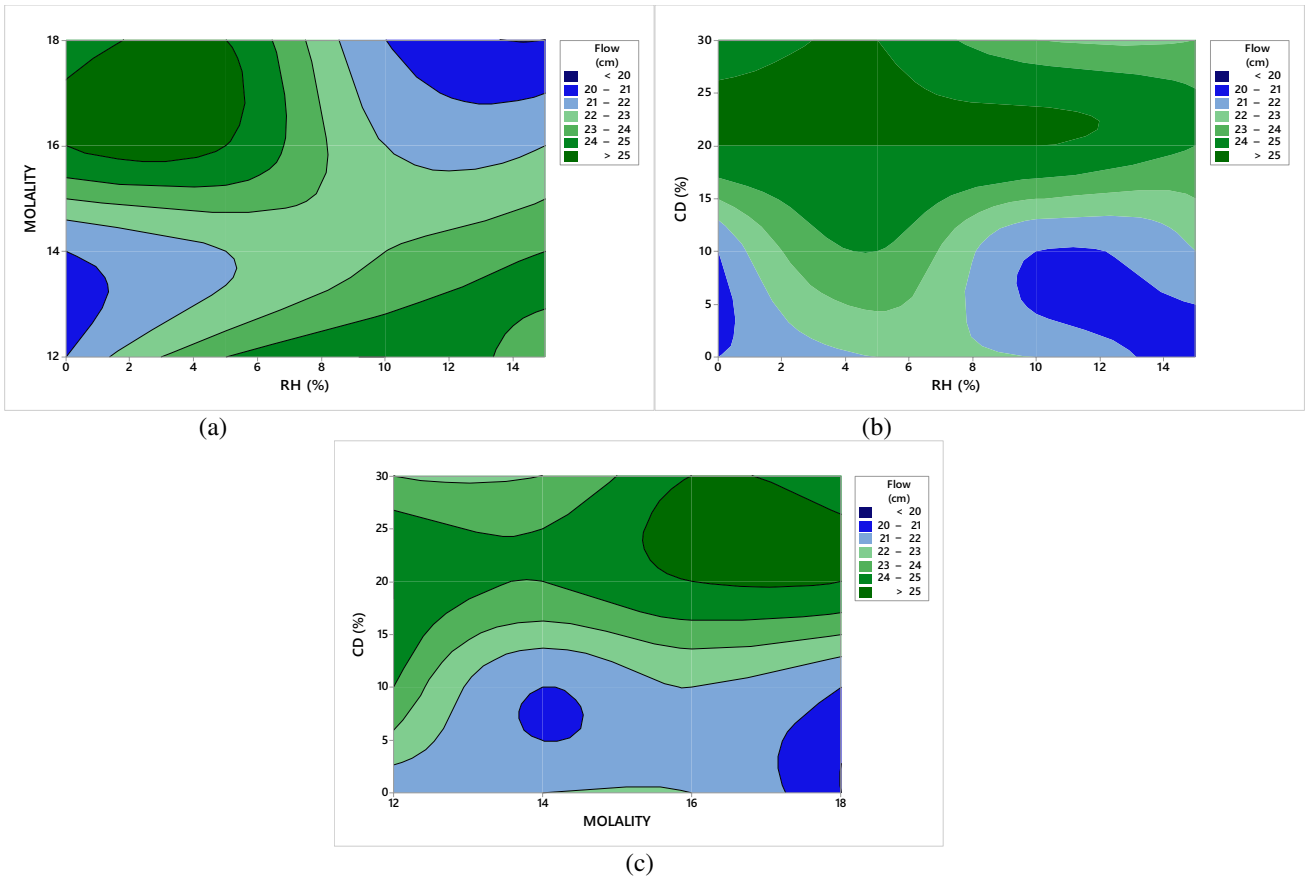

Fig. 3 Variation in spreading diameter according to parameters used

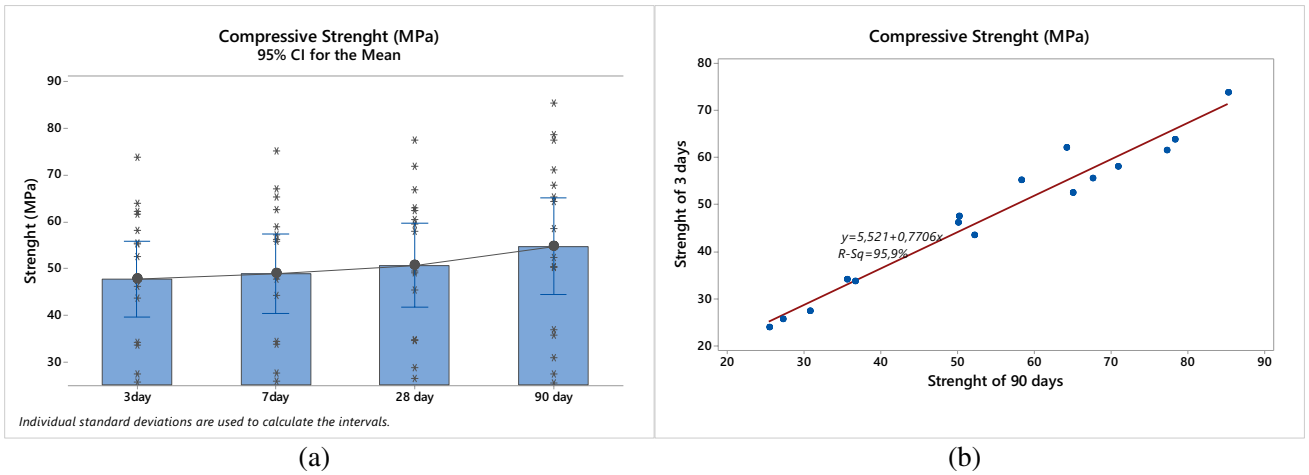

Fig. 4 Compressive strength-range distribution at every stage of testing

concrete without using RHA or CD instead of GBFS, high strength (≥ 60 MPa) was reached at 12 molality, while high strength (≥ 75 MPa) was reached at 18 molality with the addition of CD. However, although the geopolymer material using CD seems to be heterogeneous, considering the unavailable variables, it has been observed that the material prepared using high molality can cause low strengths at the increased CD rate.

The reason for the change in strengths is that heavy metal concentration changes (Table 3) the compressive

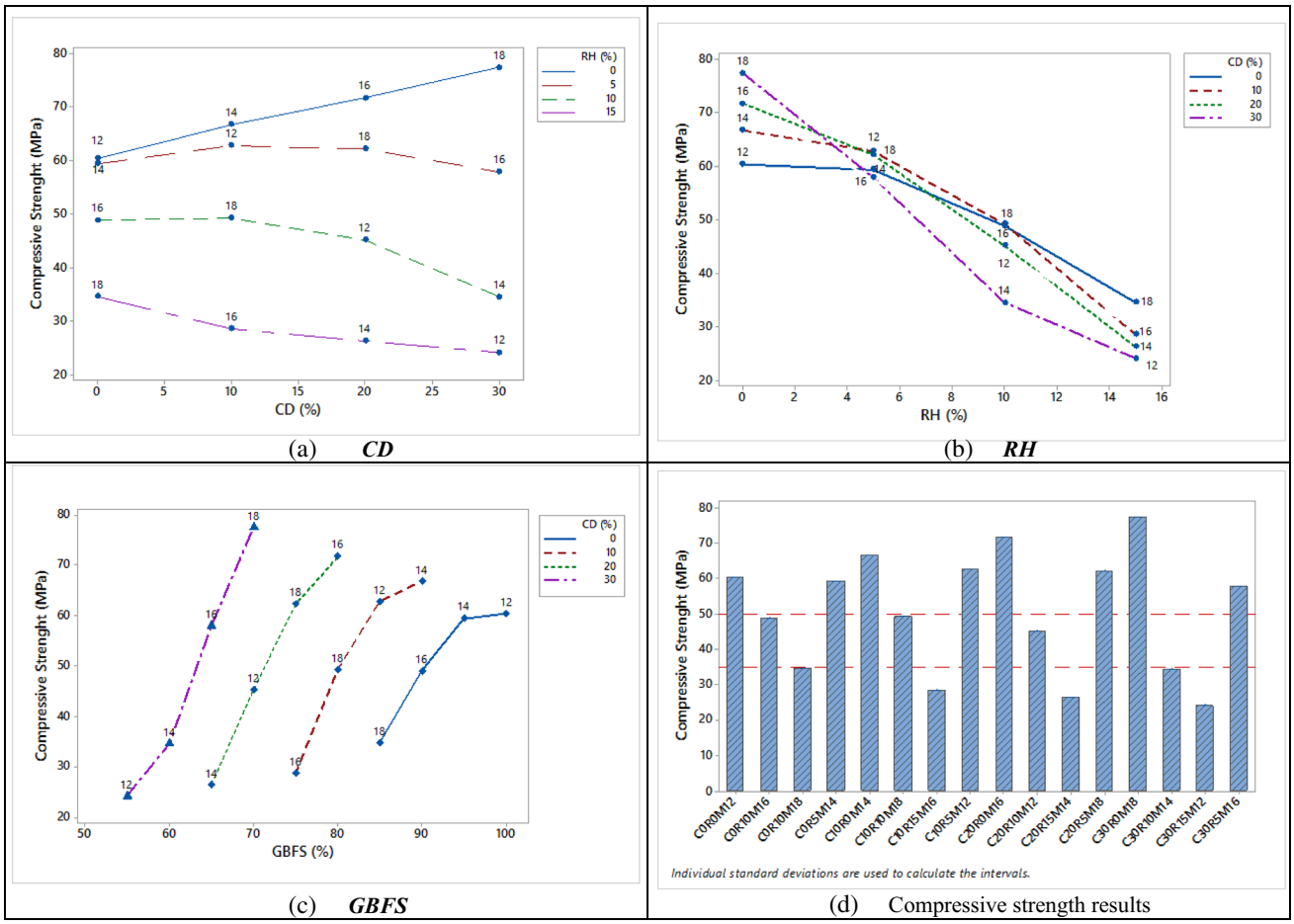

Fig. 5 Mineral admixtures impact on compressive strength results

strength of geopolymers. The dissolution of silica and alumina particles in the geopolymerization process depends on the molality of NaOH. The higher the molality of NaOH, the higher the dissolution of the silicon and aluminum particles and, consequently, the higher the strength of their mixture. Increasing NaOH molality may also cause a marginal decrease in compressive strength, which may be due to blockage of hydroxide ions (OH–) in the mixture due to high molality (Temuujin et al. 2011). This is because excessive NaOH content leaches high amounts of SiO from RHA than CD or GBFS, and inhibits the rearrangement of Si and Al (Suksiripattanapong et al. 2017). Also another cause of strength changes is the increased water:solid ratios by adding water to the mixtures to facilitate their workability with alkaline liquids, which reduces the concentration of the alkaline activator and consequently reduces the strength. The negative impact of water on geopolymerization has also been reported elsewhere (Nath and Sarker 2017; Jithendra and Elavenil 2020).

Flexural strength

The flexural strength of geopolymer concretes prepared with the Taguchi L16 matrix is shown in Table 5 and changes in Fig. 6. Flexural strength was 3.17 MPa in the 14-molality group using 10% CD without RHA, the highest flexural strength value. The lowest values were 0.38 MPa for 10% CD and 5% RHA at 12 molality and 0.40 MPa for 30% CD and 15% RHA at 12 molality. The fact that the lowest values were at 12 molality and in the RHA groups caused a marginal decrease in flexural strength, due to the decrease in NaOH molality. Flexural strength of the geopolymer concrete was low for reasons similar to those of compressive strength. In addition, the negative effects of RHA use (Fig. 6d) revealed that the hot water cure or mineral materials used in this study should be used carefully in studies where flexural strength is important. Although the effects of the materials used were variable, the 3-day results provided approximately 90% of the 90-day final strengths, and

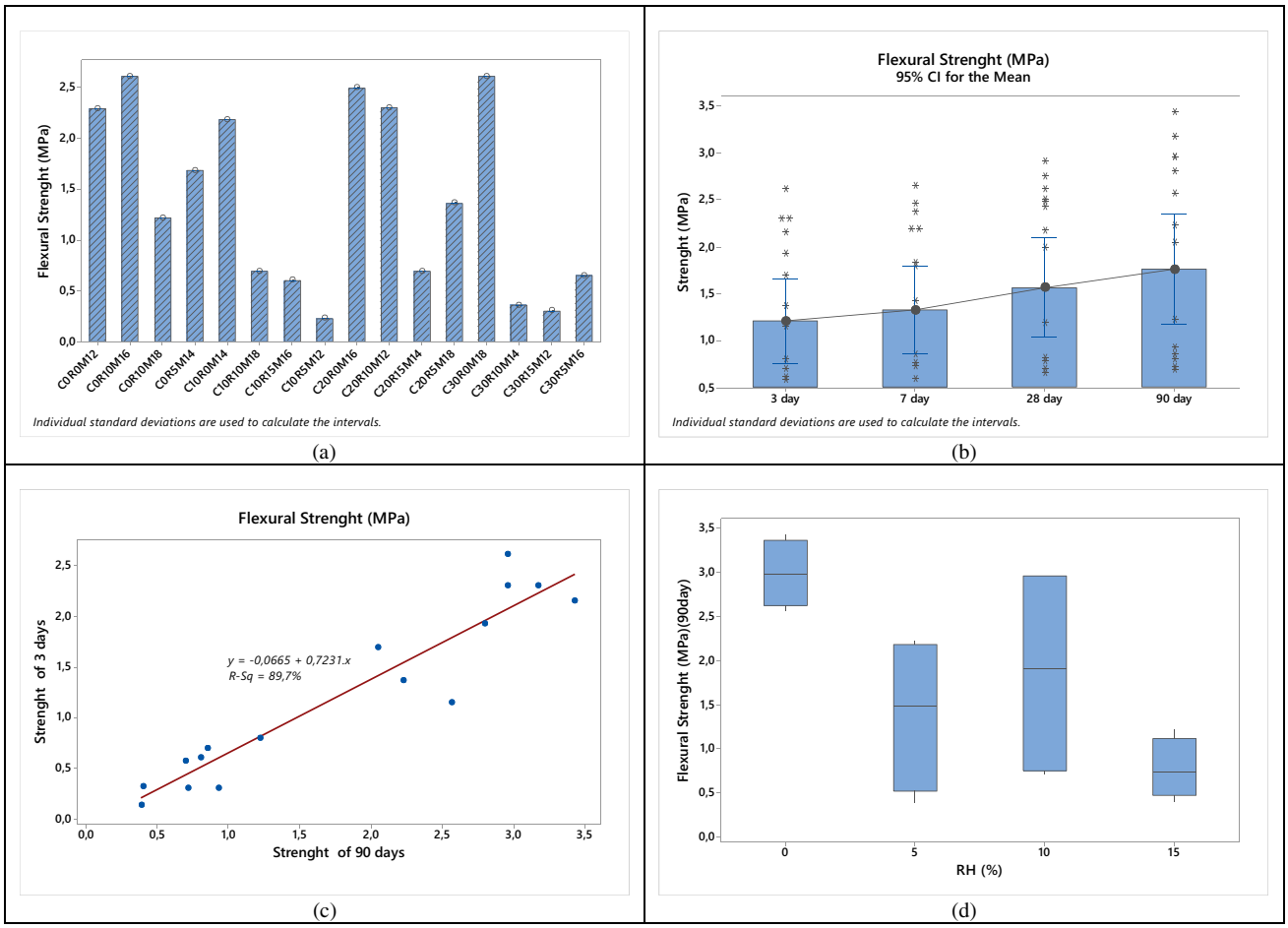

Fig. 6 Flexural strength-range distribution at every stage of testing

that there was a statistically strong regression relationship of 89.5%.

Determine of density, absorption, voids, and capilarity

The test results for density, percent absorption, percent voids, and capilartity in hardened concrete in accordance with ASTM C642 (ASTM C642 1997) are shown in Table 6.

The apparent and dry density of geopolymer concretes cured with hot water are presented in Table 6. Apparent density was 2311–2530 kg m^{-3} and dry bulk density 1752–2027 kg m^{-3}. The apparent densities of the geopolymer concretes were in good agreement with the ordinary PC (2155–2560 kg m^{-3}) densities specified in the American Concrete Institute Building Code (2014). Considering the general changes in apparent density based on molality, CD, and RHA parameters (Fig. 7a), the increase in molality varied according to the density molality used, and did not show a linear increase or decrease. In addition, if RHA were not used, only CD, density was 2300–2350 kg m^{-3}. When up to 10% RHA was used with CD and RHA, density increased, but when 15% RHA was used, density decrease. This situation is compatible with void volumes approaching 30% with increasing RHA usage (Fig. 7b). This is because the amount of fine material entering the mixture with increasing RHA decreases its compactness.

The effect of the molality on the density and the effect of the capillarity on the results (Fig. 7c) were the same, and the changes in capillarity remained almost the same due to the increased break. However, when using only CD in the mixtures, capillarity was measured at an average of 0.3 cm, while capillarity of ≥ 1 was found depending on the use of increasing RHA in the mixtures. In other words, capillarity increased with the use of RHA, which is rich in SiO_2 content, and there was no change in capillarity due to the changing molality in the use of CD containing less SiO_2 (Nuaklong et al. 2020). This is explained by the fact that although the porosity may decrease with the use of SiO_2-rich materials, increasing SiO_2/Al_2O_3 ratios tend to increase. The water absorption rate (Fig. 7d) was 6.17–15.88%. The highest water absorption was 15.88% for 20% CD and 10% RHA at 12 molality, while the lowest value was with 30% CD and

Table 6 Water absorption rate, void, capillarity, and apparent density

Mix code	Absorption after immersion (%)	Volume of permeable voids (%)	Bulk density, dry (kg m^{-3})	Bulk density after immersion kg m^{-3})	Bulk density after immersion and boiling (kg m^{-3})	Apparent density (kg m^{-3})	Capilarity (cm)
C0R0M12	6.90	15.34	1993.52	2131.13	2146.92	2355.26	0.33
C0R5M14	7.02	15.39	1993.59	2133.51	2147.51	2356.36	0.37
C0R10M16	13.42	28.21	1958.58	2221.32	2240.72	2429.40	0.47
C0R10M18	11.58	26.20	1817.72	2027.99	2137.63	2464.43	1.15
C10R0M14	6.36	13.95	2027.34	2156.15	2169.85	2356.69	0.27
C10R5M12	13.12	25.43	1828.10	2067.82	2082.36	2451.43	0.30
C10R10M18	11.49	22.20	1854.86	2067.91	2076.86	2384.51	1.40
C10R15M16	14.00	25.75	1801.82	2054.00	2059.36	2426.88	1.60
C20R0M16	6.65	14.45	1976.14	2107.34	2141.95	2311.01	0.27
C20R5M18	13.00	25.74	1832.43	2070.01	2091.13	2467.44	0.63
C20R10M12	15.88	30.72	1752.87	2031.28	2080.62	2530.09	0.70
C20R15M14	14.75	26.66	1773.61	2035.27	2065.01	2418.79	1.20
C30R0M18	6.17	14.29	1982.29	2104.56	2125.20	2313.12	0.30
C30R5M16	13.65	25.86	1821.93	2070.68	2083.48	2457.46	1.20
C30R10M14	13.77	25.29	1802.08	2050.26	2103.10	2412.24	1.30
C30R15M12	14.61	26.05	1762.51	2019.97	2024.18	2383.70	1.60

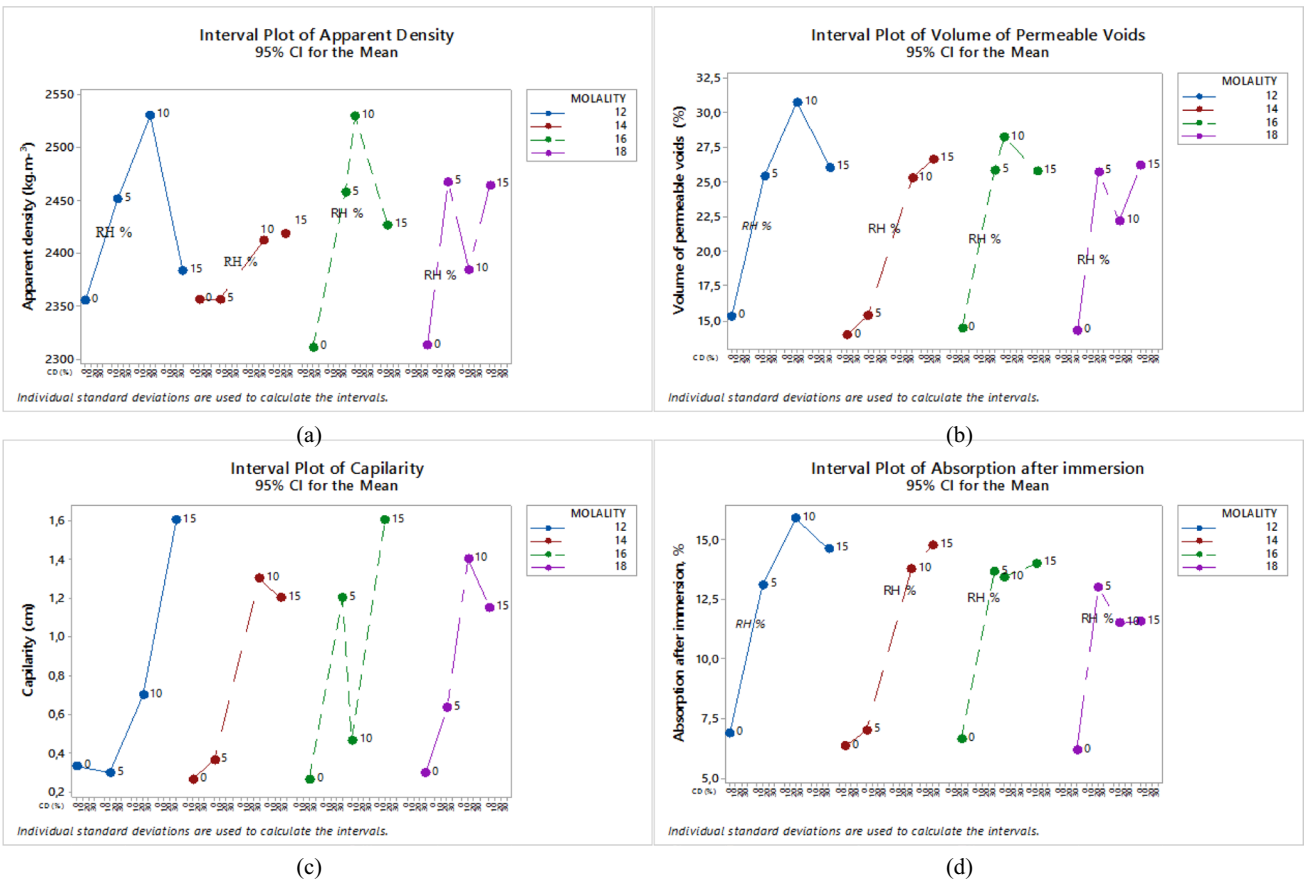

Fig. 7 The effect of mineral additives on water absorption rate (**a**), voids (**b**), capillarity (**c**), and apparent density (**d**)

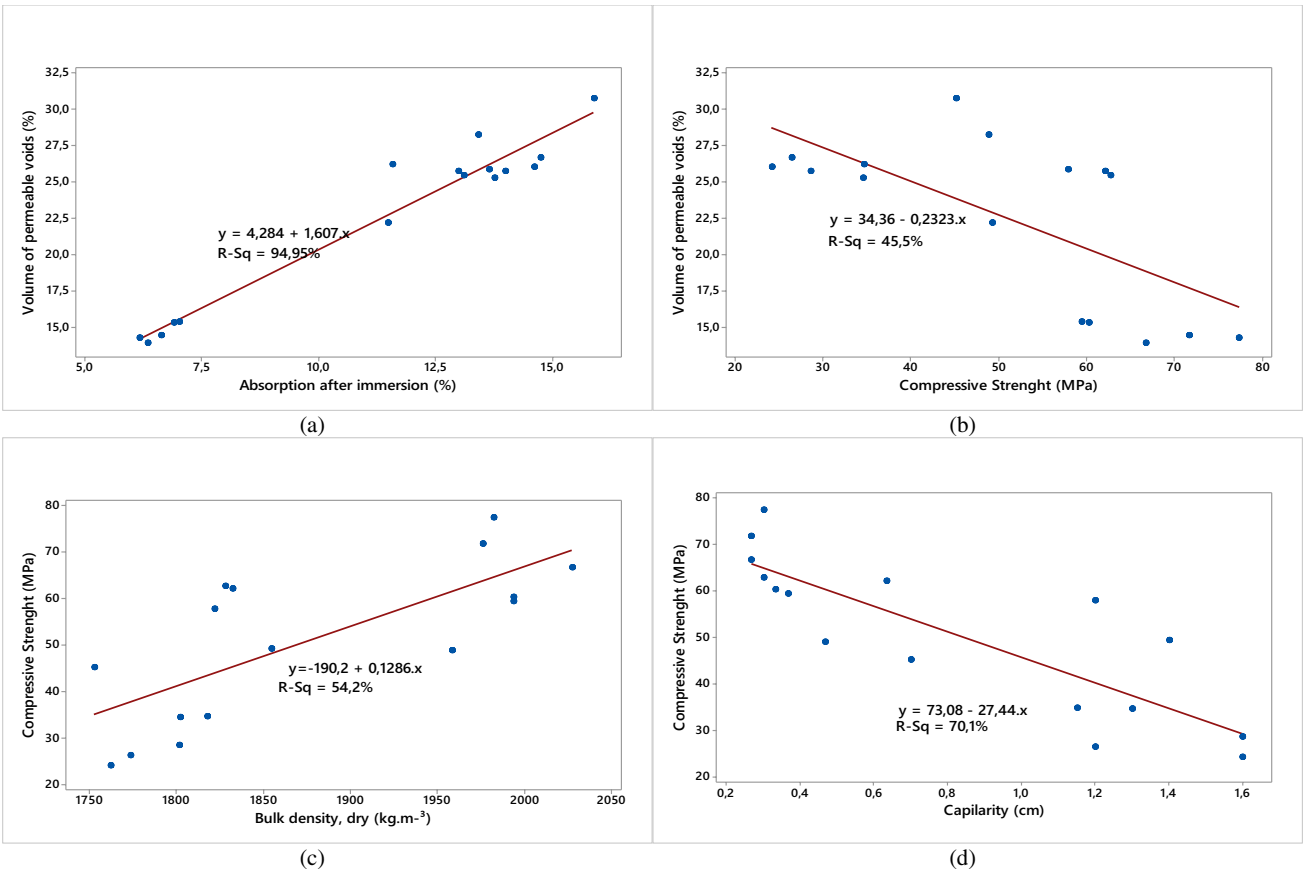

Fig. 8 Regression relationships in geopolymer concretes

Table 7 Compressive strength and mass loss rate results for mixtures

Mix code	25 °C	300 °C		450 °C		600 °C	
	CS* (MPa)	CS (MPa)	Ml (%)	CS (MPa)	Ml (%)	CS (MPa)	Ml (%)
C0R0M12	60.33	63.48	6.10	56.85	15.91	45.74	32.34
C0R5M14	59.42	61.16	6.07	50.32	22.72	48.88	24.93
C0R10M16	48.91	43.60	12.97	29.96	40.21	6.40	87.23
C0R10M18	34.70	27.00	26.40	26.33	28.22	14.77	59.72
C10R0M14	66.74	72.32	6.47	68.86	10.94	41.99	45.70
C10R5M12	62.80	58.97	8.15	48.42	24.57	17.01	73.50
C10R10M18	49.30	39.37	21.58	28.08	44.06	10.57	78.95
C10R15M16	28.62	20.76	32.51	20.16	34.45	8.07	73.76
C20R0M16	71.71	78.38	2.55	75.70	3.42	52.09	33.54
C20R5M18	62.16	53.28	24.91	29.07	59.03	42.88	39.57
C20R10M12	45.21	40.58	22.27	34.46	33.99	3.64	93.02
C20R15M14	26.40	17.05	37.43	14.84	45.56	9.73	64.30
C30R0M18	77.40	61.98	27.34	55.46	34.99	55.64	34.78
C30R5M16	57.90	43.00	26.25	31.72	45.61	13.05	77,62
C30R10M14	34.55	28.36	20.35	26.06	26.82	5.18	85.45
C30R15M12	24.18	16.73	34.29	15.79	38.00	4.72	81.45

CS compressive strength, Ml mass lose rate

*28-day samples results

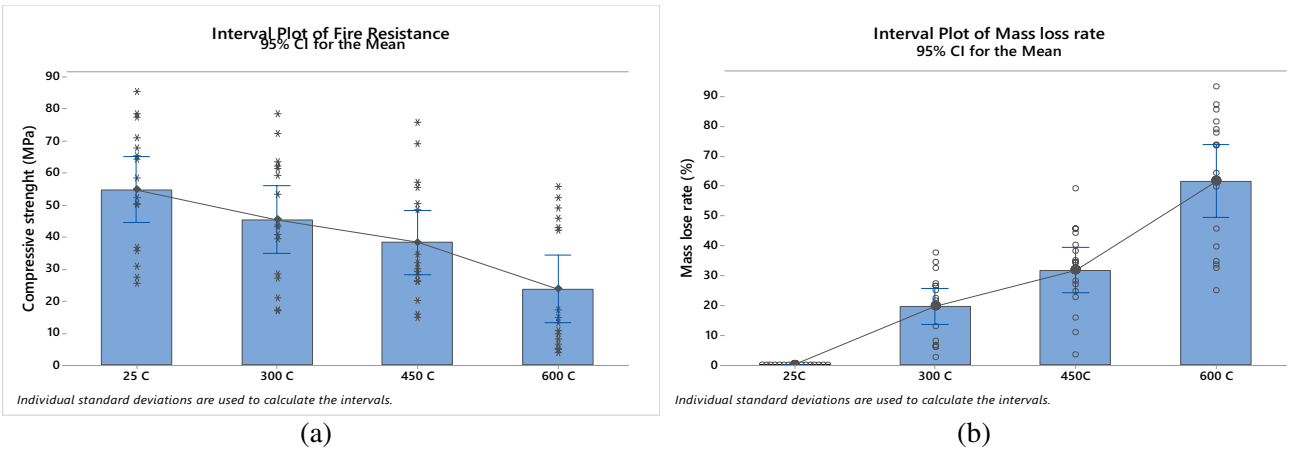

Fig. 9 Changes at high temperature: **a** compressive strength and **b** mass loss rate

0 RHA at 18 molality. The material used and the molality had an effect on the water absorption rate.

Important regression relationships were examined: absorption with void (Fig. 8a), void with compressive strength (Fig. 8b), dry bulk density with compressive strength (Fig. 8c), and capillarity with compressive strength (Fig. 8d). A strong relationship ($R^2 = 94.95\%$) occurred between void and absorption, with absorption increased in direct proportion to increasing gap. However, when the relationship between compressive strength and void

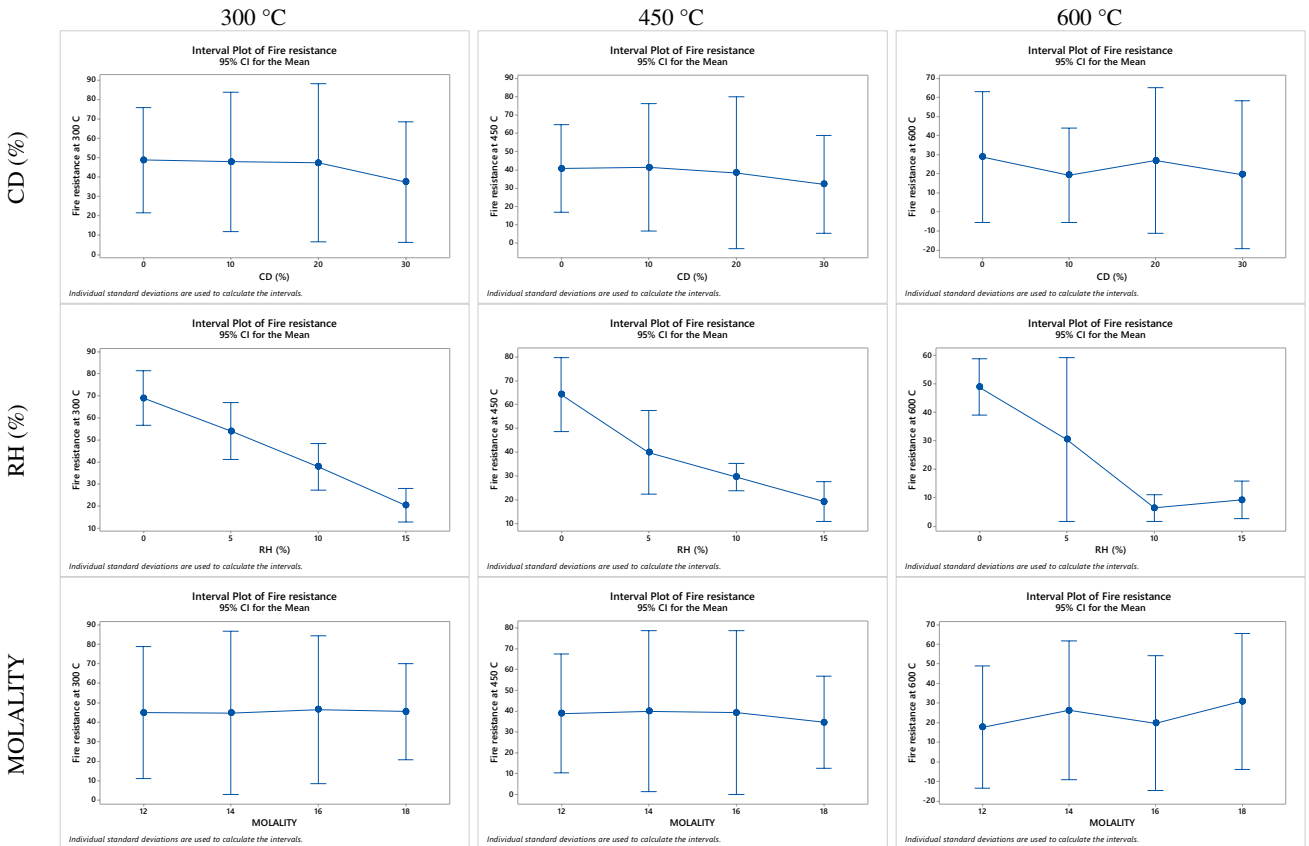

Fig. 10 The effect of CD, RHA, and molality on compressive strenght at high temperature

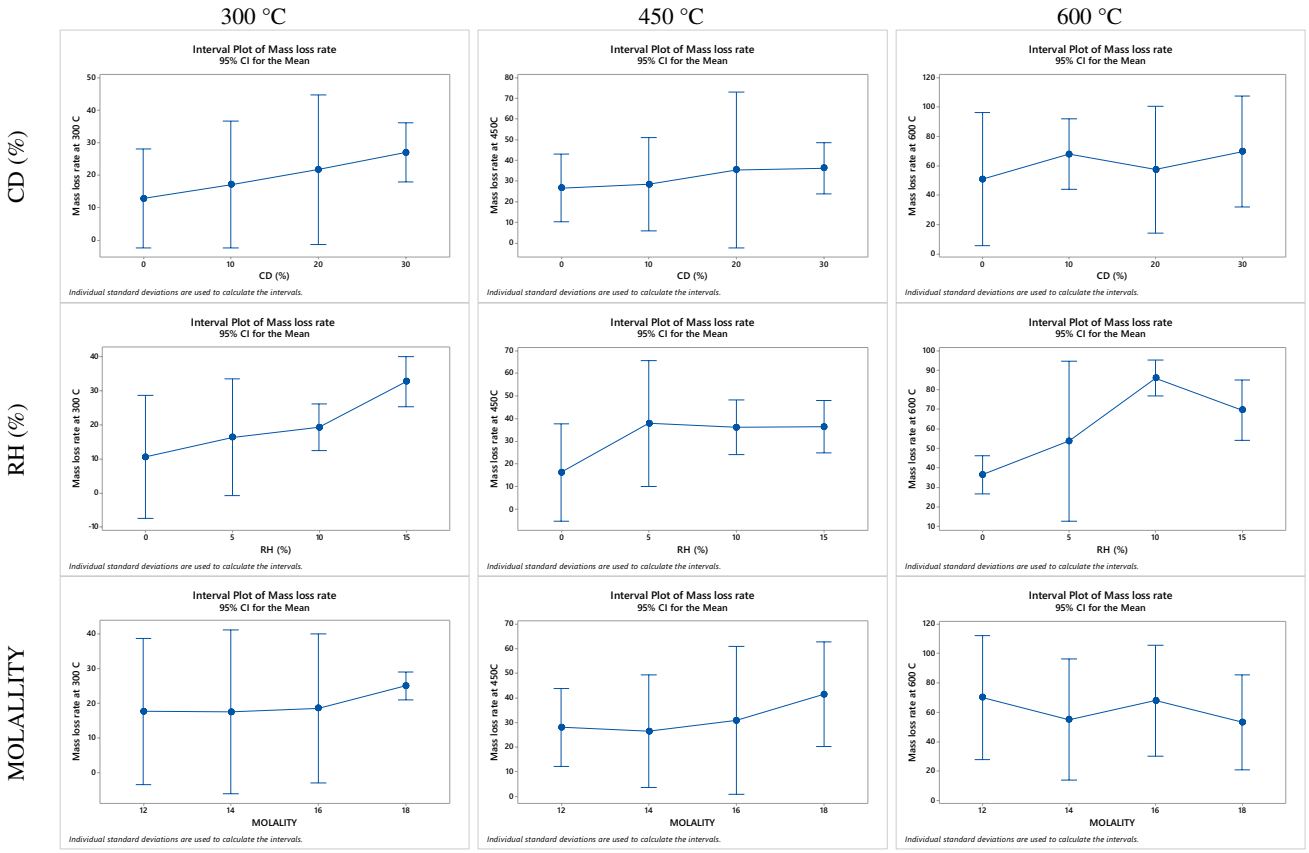

Fig. 11 The effect of CD, RHA, and molality on mass loss rate at high temperature

($R^2 = 45.5\%$) was examined, the strength decreased with increasing void. This can be explained by the fact that the materials used in some groups cannot bond enough and weak interfaces are formed. Similar situations were seen for the relationship between compressive strength and bulk density (Fig. 8c) and capillarity and compressive strength (Fig. 8d). However, in the relationship between the regression analysis results in geopolymer concretes and the other data, the $R^2 \geq 85\%$ expected by the researchers revealed situations that were incompatible with one another and therefore

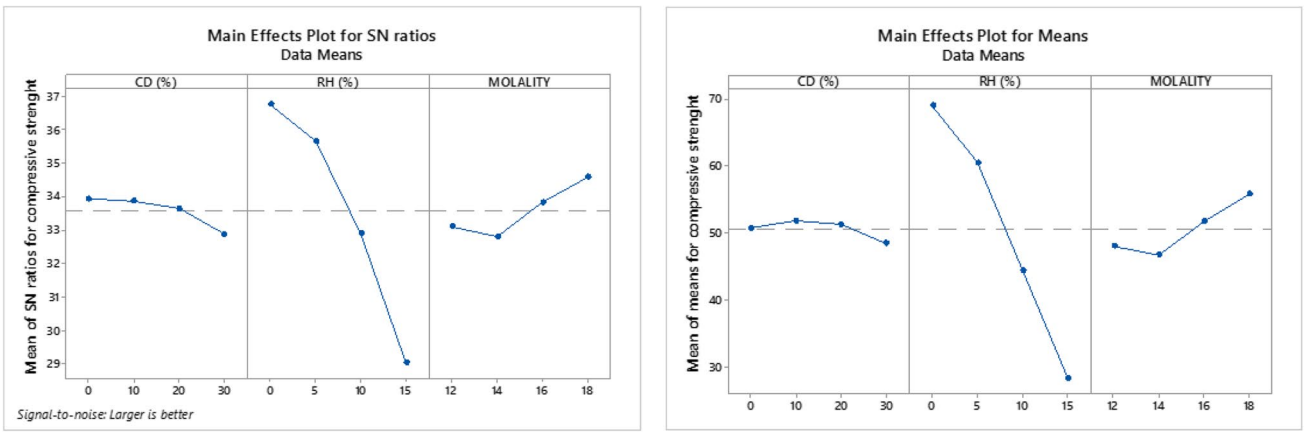

Fig. 12 Taguchi optimization S:N ratios and control factor graphs for compressive strength

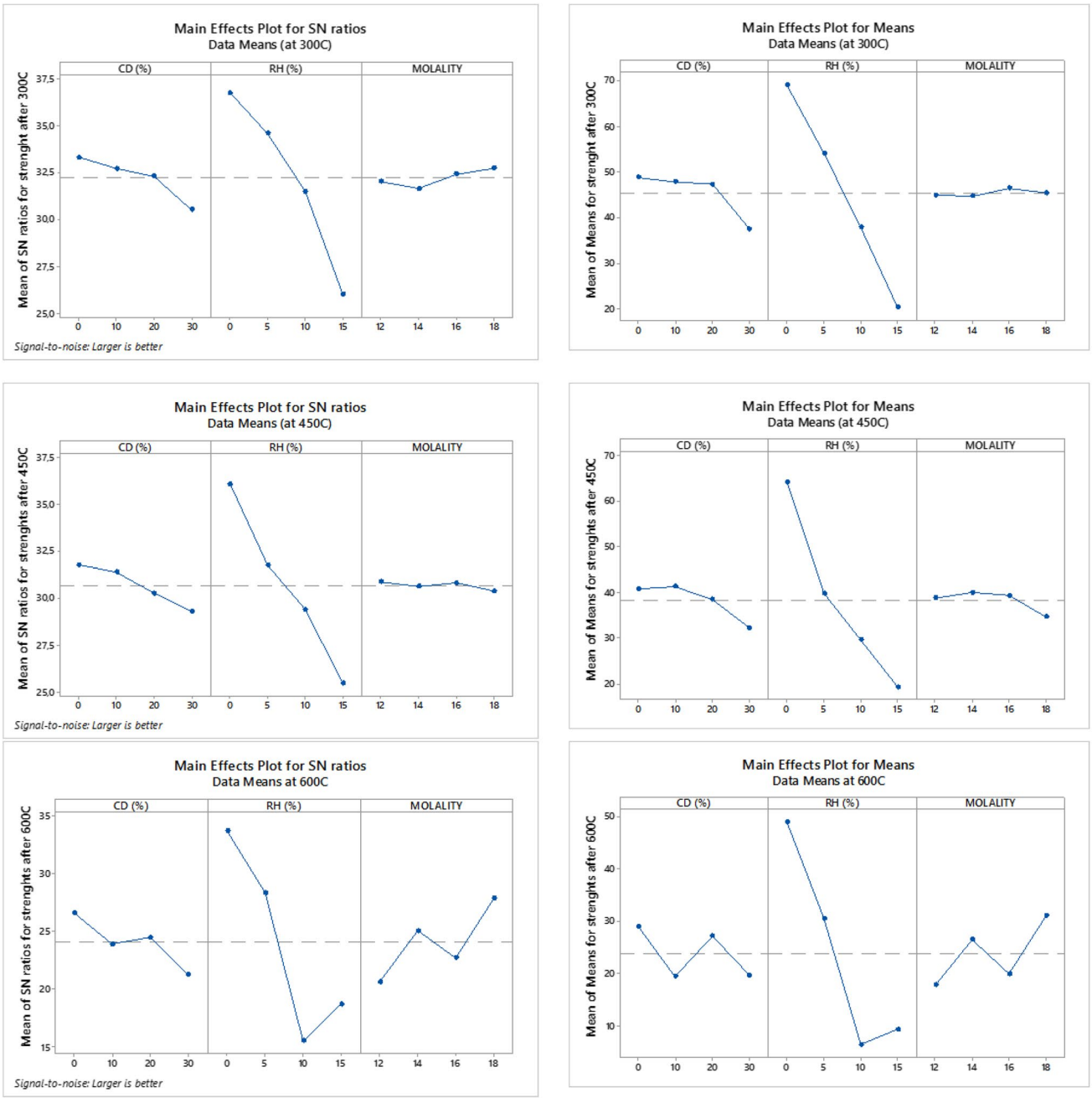

Fig. 13 Taguchi optimization S:N ratios and control factor graphs for strength and high temperatures

unexplained for some results. This is an indication that continued geopolymer research is important in order to obtain predictable results.

Fire resistance

Fire resistance–testing results are shown in Table 7.

Samples exposed to temperatures of 300 °C, 450 °C, and 600 °C showed strength loss (Fig. 9). At 300 °C, strength for all groups ranged 16.73–78.38 MPa. The lowest strength was obtained in the group prepared with 30% CD and 15% RHA at 12 molality, and the highest in the group using 20% CD at 16 molality: 14.84 MPa and 75.70 MPa at 450 °C, and 3.64 and 55.64 MPa at 600 °C, respectively. At 300 °C, the maximum loss occurred in the group with 20% CD and 15% RHA at 14 molality — 35.41%. Losses were found in the group prepared with CD 20%, RHA 5%, and 18 molality at 450 °C (53.23%) and

Table 8 Optimal results and validation experiments for control factors 24

Temperature	Test	Taguchi optimization	Predicted value			Real value		
			CD	RHA	M	CD	RHA	M
25 °C	Compressive strength	Level	2	1	4	2	1	4
		Value	10	0	18	10	0	18
		SN ratio	38,044			–		
		Result (MPa)	75.51			73.25		
300 °C	Compressive strength	Level	1	1	3	1	1	3
		Value	0	0	16	0	0	16
		SN ratio	38.05			–		
		Result (MPa)	73.54			68.14		
	Mass loss rate	Level	1	1	3	1	1	3
		Value	0	0	16	0	0	16
		SN ratio	−12.23			–		
		Result (%)	2.62			2.97		
450 °C	Compressive strength	Level	2	1	2	2	1	2
		Value	10	0	14	10	0	14
		SN ratio	36.74			–		
		Result (MPa)	69.11			68.86		
	Mass loss rate	Level	2	1	2	2	1	2
		Value	10	0	14	10	0	14
		SN ratio	−19.74			–		
		Result (%)	6.02			10.94		
600 °C	Compressive strength	Level	1	1	4	1	1	4
		Value	0	0	18	0	0	18
		SN ratio	40.06			–		
		Result (MPa)	61.23			54.45		
	Mass loss rate	Level	1	1	4	1	1	4
		Value	0	0	18	0	0	18
		SN ratio	−28.14			–		
		Result (%)	17.67			19.21		

for that with CD 20% and RHA 10% at 12 molality, with maximum loss of 91.95% at 600 °C. Five groups showed increased strength at 300 °C: 5.2% to 12 molality without any CD or RHA added, 14 molality with 5% RHA additive, 14 molality with 10% CD additive, and 16 molality with 20% CD additive. Although there was a loss of strength when the temperature was increased from 300 to 600 °C (Fig. 10), the positive effect of added CD and RHA was very low. This is because high temperatures accelerate the bond-breaking process in the geopolymer matrix. Damage and loss of strength appear higher in samples containing high levels of calcium, which is the product of calcium carbonate decomposition, which causes cracks to develop by causing an increase in volume. This phenomenon can be caused by two opposing processes occurring in the samples as the temperature increases: power gain from continuing geopolymerization or loss of power due to thermal mismatch to resist temperature rise (Huseien et al. 2018).

The change in weight loss caused by high temperatures in geopolymers is on average 20% at 300 °C, and this mass loss has been found to cause an average loss of 60% with increasing temperature (Fig. 9b). High-temperature effects were analyzed according to RHA, CD, and molality (Fig. 11). At 300 °C, the disjunction did not cause a significant change in mass loss rate (excluding 18 molality), and was the cause of an average loss of 20%. At 450 °C and 600 °C temperatures, this ratio remained at 35% and 60%, respectively, and showed a homogeneous effect. However, CD used at a high rate caused 10–30% mass loss at 450 °C and an average 65% mass loss at 600 °C. It was observed that RHA used at a lower rate caused an average 10–35% loss at 450 °C and 70% loss at 600 °C. Many researchers have tested concrete reactions at high temperatures and observed that in the initial phase (up to 400 °C), there is relatively little loss of mass, but an increase in strength and then a tendency toward decreased strength and increased mass loss. The mass loss corresponding to the evaporation of free and

physically bound water in the geopolymer gel assays is reported to occur below 250 °C (Yang et al. 2017).This is explained by the fact that the chemical bonds formed as a result of geopolymerization in geopolymers deteriorate more quickly and create a weaker bond with the effect of temperature. Ameri et al. recommended two opposite processes for changes in matrix structure under exposure to high temperatures (Ameri et al. 2019): matrix damage due to thermal incompatibility of the components, or the process of strengthening by further hydration or geopolymerization, which densifies the matrix.

4.3. Taguchi optimization

Taguchi analysis for strengths

In determining the most ideal mixture based on the results obtained by using Taguchi L16 test matrix, firstly, optimum results of compressive strength and secondly compressive strength and mass lose rate according to after the high temperatures are given in Figs. 12 and 13 and the optimum levels of these results are given in Table 8.

When the results are examined, there may sometimes be any of the existing experiments in the optimizations, but there may be mixtures other than those tested in this study. In this study, 73.25 MPa strength was obtained upon verification testing in the 10% CD, 0 RHA, and 18 molality group, which was not found in Taguchi L16 matrix, and determined as the optimum result for compressive strength. Optimization results in the investigation of the effects of high temperatures on strength and mass loss, both strength and mass loss results, were obtained for the same groups. Among these groups, 10% CD, 0 RHA, and 14 molality groups determined at 450 °C were found in the same group with the Taguchi L16 matrix, and results close to the predicted values were obtained. In other results achieved in different groups, Taguchi L16 matrix and verification data are given in Table 8.

Conclusions

The following conclusions were obtained in this study:

- The use of more than 10% CD in geopolymer concretes has led to a significant increase in dynamic flow. In addition, the use of RHA and molalite has a statistically variable effect on dynamic flow, with R-Sq values ranging from 7.4 to 15.76%. Accordingly, for very high viscosity, CD has a greater effect than RHA and mollite.
- With the increasing use of CD in geopolymer concrete production, 2311–2350 kg m^{-3} decreasing densities have been obtained. The use of RHA, which was prepared in different mollites but increased depending on the rate, increased the densities between 2350 and 2530 kg m^{-3} degradation. High density value was reached in 12 mollites.
- Volume of permeable voids decreased by 2.5% with increased molality, and the voids was similar in CD use. However, increased RHA use has resulted in a nearly 100% increase in the volume of permeable voids.
- RHA had a greater effect on the increase in water absorption rates than CD. Geopolymers with high water absorption rates at high levels of porosity in conjunction with voids were obtained.
- The compressive strength of increasing molality decreased, but if only CD was used in the mixtures, compressive strengths of > 70 Mpa were obtained. In addition, with the decrease in molality, it did not cause a significant loss in strength when 10% RHA is used. However, in the groups prepared with 16 and 18 molality, there was a loss of strength up to 50% when using RHA over 10%.
- The effect of CD was more than that of RHA in geopolymers under high temperatures, rather than breakage. The material that is effective in both strength and mass loss is CD.
- The Taguchi method showed that compressive strength can be obtained at different molality values such that CD does not exceed 10% in mass loss. It has also been seen that it is advantageous to use the Taguchi method to investigate the effect of different additives on geopolymer concretes.

Finally, low porosity and water absorption rates, strengths > 50 MPa can be obtained. The use of CD is more effective on compressive strength than RHA, and it is advantageous to use up to 30% CD without RHA to attain strength > 70 MPa. In geopolymers to be produced using RHA, it should be used at rates not exceeding 5% for high strength. In addition, if RHA and CD are used in geopolymer materials, materials of sufficient strength similar to PC concretes can be obtained.

Author contribution Selçuk Memiş contributed to writing of article and literature review. Mohamed Ahmed Mohamed BILAL performed the experiments and anayzed the results.

Data availability Not applicable.

Declarations

Ethics approval and consent to participate Not applicable.

Consent for publication Not applicable.

Competing interests The authors declare no competing interests.

References

Abbasi SM, Ahmadi H, Khalaj G, Ghasemi B (2016) Microstructure and mechanical properties of a metakaolinite-based geopolymer nanocomposite reinforced with carbon nanotubes. Ceram Int 42:15171–15176. https://doi.org/10.1016/j.ceramint.2016.06.080

Abdel-ghani NT, Elsayed HA, Abdelmoied S (2018) Geopolymer synthesis by the alkali-activation of blastfurnace steel slag and its fire-resistance. HBRC J 14:159–164. https://doi.org/10.1016/j.hbrcj.2016.06.001

Abdullah, Hussin, Zakaria M (2006) Pofa : a potential partial cement replacement material in aerated concrete. 6th Asia Pacific Struct Eng Constr (APSEC 2006) 5–6

Adesanya DA, Raheem AA (2009) Development of corn cob ash blended cement. Constr Build Mater 23:347–352. https://doi.org/10.1016/j.conbuildmat.2007.11.013

Akbar A, Farooq F, Shafique M et al (2021) Sugarcane bagasse ash-based engineered geopolymer mortar incorporating propylene fibers. J Build Eng 33:101492. https://doi.org/10.1016/j.jobe.2020.101492

Albidah AS (2021) Effect of partial replacement of geopolymer binder materials on the fresh and mechanical properties: a review. Ceram Int. https://doi.org/10.1016/j.ceramint.2021.02.127

Alnkaa A, Yaprak H, Memis S, Kaplan G (2018) Effect of different cure conditions on the shrinkage of geopolymer mortar. Int J Eng Res Dev 14:51–55

Alsubari B, Shafigh P, Jumaat MZ (2016) Utilization of high-volume treated palm oil fuel ash to produce sustainable self-compacting concrete. J Clean Prod 137:982–996. https://doi.org/10.1016/j.jclepro.2016.07.133

Altoubat S, Badran D, Junaid MT, Leblouba M (2016) Restrained shrinkage behavior of self-compacting concrete containing ground-granulated blast-furnace slag. Constr Build Mater 129:98–105. https://doi.org/10.1016/j.conbuildmat.2016.10.115

Ambedkar B, Alex J, Dhanalakshmi J (2017) Enhancement of mechanical properties and durability of the cement concrete by RHA as cement replacement: experiments and modeling. Constr Build Mater 148:167–175. https://doi.org/10.1016/j.conbuildmat.2017.05.022

Ameri F, Shoaei P, Alireza S, Behforouz B (2019) Geopolymers vs. alkali-activated materials (AAMs): a comparative study on durability, microstructure, and resistance to elevated temperatures of lightweight mortars. Constr Build Mater 222:49–63. https://doi.org/10.1016/j.conbuildmat.2019.06.079

American Concrete Institute Building Code (2014) 318-14: Building code requirements for structural concrete and commentary

Amran M, Debbarma S, Ozbakkaloglu T (2021) Fly ash-based eco-friendly geopolymer concrete : a critical review of the long-term durability properties. Constr Build Mater 270:121857. https://doi.org/10.1016/j.conbuildmat.2020.121857

Annakoa MAI, Memis S, Kaplan G, Yaprak H (2019) Effect of Adding glass powder in geopolymer concrete. In: International Congress on Engineering and Life Science, ICELIS. pp 480–484

Arnold MC, de Vargas AS, Bianchini L (2017) Study of electric-arc furnace dust (EAFD) in fly ash and rice husk ash-based geopolymers. Adv Powder Technol 28:2023–2034. https://doi.org/10.1016/j.apt.2017.05.007

Assi LN, Eddie Deaver E, Ziehl P (2018) Effect of source and particle size distribution on the mechanical and microstructural properties of fly ash-based geopolymer concrete. Constr Build Mater 167:372–380. https://doi.org/10.1016/j.conbuildmat.2018.01.193

(2004) ASTM C1585–04, Standard Test method for measurement of rate of absorption of water by hydraulic-cement concretes,

ASTM C 136 / C136M-19 (2014) Standard test method for sieve analysis of fine and coarse aggregates. ASTM Int

ASTM C1437–20 (2020) Standard test method for flow of hydraulic cement mortar. ASTM Int

ASTM C642 (1997) Standard Test method for density , absorption , and voids in hardened concrete 1. 1–3

(2017) ASTM E2748–12a, Standard Guide for fire-resistance experiments,

ASTM E831 (2014) Standard test method for linear thermal expansion of solid materials by thermomechanical analysis,

Bagheri A, Nazari A (2014) Compressive strength of high strength class C fly ash-based geopolymers with reactive granulated blast furnace slag aggregates designed by Taguchi method. Mater Des 54:483–490. https://doi.org/10.1016/j.matdes.2013.07.035

Bernal SA, Rodríguez ED, de Gutiérrez R et al (2011) Mechanical and thermal characterisation of geopolymers based on silicate-activated metakaolin/slag blends. J Mater Sci 46:5477. https://doi.org/10.1007/s10853-011-5490-z

Cannio M, Billong N (2017) Substitution of sodium silicate with rice husk ash-NaOH solution in metakaolin based geopolymer cement concerning reduction in global warming. J Clean Prod 142:3050–3060. https://doi.org/10.1016/j.jclepro.2016.10.164

Charkhtab S, Madandoust R, Jamshidi M, Nikbin IM (2021) Mechanical properties of fly ash-based geopolymer concrete with crumb rubber and steel fiber under ambient and sulfuric acid conditions. Constr Build Mater 281:122571. https://doi.org/10.1016/j.conbuildmat.2021.122571

Cheah CB, Ramli M (2011) The implementation of wood waste ash as a partial cement replacement material in the production of structural grade concrete and mortar: an overview. Resour Conserv Recycl 55:669–685

Corinaldesi V, Fava G, Ruello ML (2010) Paper mill sludge ash as supplementary cementitious material. In: 2nd International Conference on Sustainable Construction Materials and Technologies. American Society of Civil Engineers, pp 85–94

Cristina M, De VAS, Bianchini L (2017) Study of electric-arc furnace dust (EAFD) in fly ash and rice husk ash-based geopolymers. Adv Powder Technol 28:2023–2034. https://doi.org/10.1016/j.apt.2017.05.007

Dadsetan S, Siad H, Lachemi M, Sahmaran M (2021) Evaluation of the tridymite formation as a technique for enhancing geopolymer binders based on glass waste. J Clean Prod 278:123983. https://doi.org/10.1016/j.jclepro.2020.123983

Darsanasiri AGND, Matalkah F, Ramli S et al (2018) Ternary alkali aluminosilicate cement based on rice husk ash, slag and coal fly ash. J Build Eng 19:36–41. https://doi.org/10.1016/j.jobe.2018.04.020

Dave SV, Bhogayata A (2020) The strength oriented mix design for geopolymer concrete using Taguchi method and Indian concrete mix design code. Constr Build Mater 262:120853. https://doi.org/10.1016/j.conbuildmat.2020.120853

Deepika S, Anand G, Bahurudeen A, Santhanam M (2017) Construction products with sugarcane bagasse ash binder. J Mater Civ Eng 29:04017189. https://doi.org/10.1061/(asce)mt.1943-5533.0001999

El-Dieb AS, Kanaan DM (2018) Ceramic waste powder an alternative cement replacement – characterization and evaluation. Sustain Mater Technol 17:e00063. https://doi.org/10.1016/j.susmat.2018.e00063

El-Gamal SMA, El-Hosiny FI, Amin MS, Sayed DG (2017) Ceramic waste as an efficient material for enhancing the fire resistance and mechanical properties of hardened Portland cement pastes. Constr Build Mater 154:1062–1078. https://doi.org/10.1016/j.conbuildmat.2017.08.040

Elyamany HE, Abd Elmoaty AEM, Elshaboury AM (2018) Setting time and 7-day strength of geopolymer mortar with various binders. Constr Build Mater 187:974–983. https://doi.org/10.1016/j.conbuildmat.2018.08.025

BS EN 196–1 (2005) British standard methods of testing cement —. 3:

(2016) TS EN 196–1. Methods of testing cement - Part 1: Determination of strength. 35

(2020) TS EN 1015–11; Methods of test for mortar for masonry - Part 11: determination of flexural and compressive strength of hardened mortar. 18

Ganesan K, Rajagopal K, Thangavel K (2007) Evaluation of bagasse ash as supplementary cementitious material. Cem Concr Compos 29:515–524. https://doi.org/10.1016/j.cemconcomp.2007.03.001

Ghafoor MT, Khan QS, Qazi AU et al (2021) Influence of alkaline activators on the mechanical properties of fly ash based geopolymer concrete cured at ambient temperature. Constr Build Mater 273:121752. https://doi.org/10.1016/j.conbuildmat.2020.121752

Gielen D, Bennaceur K, Kerr T, et al (2007) IEA, Tracking ındustrial energy efficiency and co2 emissions

Görhan G, Kürklü G (2014) The influence of the NaOH solution on the properties of the fly ash-based geopolymer mortar cured at different temperatures. Compos Part B Eng 58:371–377. https://doi.org/10.1016/j.compositesb.2013.10.082

Habert G, D'Espinose De Lacaillerie JB, Roussel N (2011) An environmental evaluation of geopolymer based concrete production: reviewing current research trends. J Clean Prod. https://doi.org/10.1016/j.jclepro.2011.03.012

Hadi MNS, Farhan NA, Sheikh MN (2017) Design of geopolymer concrete with GGBFS at ambient curing condition using Taguchi method. Constr Build Mater 140:424–431. https://doi.org/10.1016/j.conbuildmat.2017.02.131

Heath A, Paine K, Mcmanus M (2014) Minimising the global warming potential of clay based geopolymers. J Clean Prod 78:75–83. https://doi.org/10.1016/j.jclepro.2014.04.046

Hu M, Zhu X, Long F (2009) Alkali-activated fly ash-based geopolymers with zeolite or bentonite as additives. Cem Concr Compos. https://doi.org/10.1016/j.cemconcomp.2009.07.006

Huseien GF, Sam ARM, Mirza J et al (2018) Waste ceramic powder incorporated alkali activated mortars exposed to elevated temperatures: performance evaluation. Constr Build Mater 187:307–317. https://doi.org/10.1016/j.conbuildmat.2018.07.226

Hwang C, Huynh T (2015) Effect of alkali-activator and rice husk ash content on strength development of fly ash and residual rice husk ash-based geopolymers. Constr Build Mater 101:1–9. https://doi.org/10.1016/j.conbuildmat.2015.10.025

IEA (2020) Cement, IEA, Paris. https://www.iea.org/reports/cement

Jithendra C, Elavenil S (2020) Influences of parameters on slump flow and compressive strength properties of aluminosilicate based flowable geopolymer concrete using Taguchi method. SILICON 12:595–602. https://doi.org/10.1007/s12633-019-00166-w

Kamseu E, Rizzuti A, Leonelli C, Perera D (2010) Enhanced thermal stability in K 2 O-metakaolin-based geopolymer concretes by Al 2 O 3 and SiO 2 fillers addition. 1715–1724. https://doi.org/10.1007/s10853-009-4108-1

Kamseu E, Beleuk à Moungam LM, Cannio M, et al (2017) Substitution of sodium silicate with rice husk ash-NaOH solution in metakaolin based geopolymer cement concerning reduction in global warming. J Clean Prod 142:3050–3060. https://doi.org/10.1016/j.jclepro.2016.10.164

Kaplan G, Yaprak H, Memiş S, Alnkaa A (2019) Artificial neural network estimation of the effect of varying curing conditions and cement type on hardened concrete properties. Buildings 9:. https://doi.org/10.3390/buildings9010010

Kaur K, Singh J, Kaur M (2018) Compressive strength of rice husk ash based geopolymer: The effect of alkaline activator. Constr Build Mater 169:188–192. https://doi.org/10.1016/j.conbuildmat.2018.02.200

Khalaj G, Hassani SES, Khezrloo A, Haratifar EAD (2014) Split tensile strength of OPC-based geopolymers: application of doE method in evaluating the effect of production parameters and their optimum condition. Ceram Int 40:10945–10952. https://doi.org/10.1016/j.ceramint.2014.03.094

Kishore K, Gupta N (2021) Materials today : proceedings mechanical characterization and assessment of composite geopolymer concrete. Mater Today Proc. https://doi.org/10.1016/j.matpr.2020.06.319

Komnitsas KA (2011) Potential of geopolymer technology towards green buildings and sustainable cities. Procedia Eng 21:1023–1032. https://doi.org/10.1016/j.proeng.2011.11.2108

Kumar M, Kumar S, Singh NB (2019) Influence of some additives on the properties of fly ash based geopolymer cement mortars. SN Appl Sci 1:1–12. https://doi.org/10.1007/s42452-019-0506-4

Liang X, Wu C, Su Y, et al (2018) Development of ultra-high performance concrete with high fire resistance. Constr Build Mater 400–412

Masi G, Rickard WDA, Vickers L et al (2014) A comparison between different foaming methods for the synthesis of light weight geopolymers. Ceram Int. https://doi.org/10.1016/j.ceramint.2014.05.108

Mayhoub OA, Nasr EAR, Ali Y, Kohail M (2020) Properties of slag based geopolymer reactive powder concrete. Ain Shams Eng J. https://doi.org/10.1016/j.asej.2020.08.013

Memis S, Kaplan G, Yildizel SA (2017a) Investigation of usability potential geopolimer concrete at animal barns. Turkish J Agric - Food Sci Technol 5:1365–1370

Memis S, Sahin S, Sirin U (2017b) Some properties of prefabricated building materials produced from ground diatomite and hydrophone clay. Pamukkale Univ J Eng Sci 23:245–249. https://doi.org/10.5505/pajes.2016.34467

Memis S, Kaplan G, Yaprak H, et al (2018) Some durability properties of alkali activated materials (AAM) produced with ceramic powder and micro calcite. Ceram - Silikaty 62:342–354. https://doi.org/10.13168/cs.2018.0030

Nath P, Sarker PK (2017) Flexural strength and elastic modulus of ambient-cured blended low-calcium fly ash geopolymer concrete. Constr Build Mater 130:22–31. https://doi.org/10.1016/j.conbuildmat.2016.11.034

Nazari A, Sanjayan JG (2015) Hybrid effects of alumina and silica nanoparticles on water absorption of geopolymers: application of Taguchi approach. Meas J Int Meas Confed 60:240–246. https://doi.org/10.1016/j.measurement.2014.10.004

Nimwinya E, Arjharn W, Horpibulsuk S et al (2016) A sustainable calcined water treatment sludge and rice husk ash geopolymer. J Clean Prod. https://doi.org/10.1016/j.jclepro.2016.01.060

Nuaklong P, Jongvivatsakul P, Pothisiri T et al (2020) Influence of rice husk ash on mechanical properties and fire resistance of recycled aggregate high-calcium fly ash geopolymer concrete. J Clean Prod 252:119797. https://doi.org/10.1016/j.jclepro.2019.119797

Nuruddin MFB, Bayuji R (2009) Optimum Mix proportioning of mirha foamed concrete using taguchi ' s approach. Apsec-Eacef 694–700

Nuruddin MF, Azmee NM, Yung CK (2014) Effect of fire flame exposure on ductile self-compacting concrete (DSCC) blended with MIRHA and fly ash. Constr Build Mater 50:388–393. https://doi.org/10.1016/j.conbuildmat.2013.09.038

Olivia M, Nikraz H (2012) Properties of fly ash geopolymer concrete designed by Taguchi method. Mater Des 36:191–198. https://doi.org/10.1016/j.matdes.2011.10.036

Omer SA, Demirboga R, Khushefati WH (2015) Relationship between compressive strength and UPV of GGBFS based geopolymer mortars exposed to elevated temperatures. Constr Build Mater 94:189–195. https://doi.org/10.1016/j.conbuildmat.2015.07.006

Onoue K, Iwamoto T, Sagawa Y (2019) Optimization of the design parameters of fly ash-based geopolymer using the dynamic approach of the Taguchi method. Constr Build Mater 219:1–10. https://doi.org/10.1016/j.conbuildmat.2019.05.177

Perera DS, Vance ER, Finnie KS, et al (2006) Disposition of water in metakaolinite based geopolymers. In: Ceramic Transactions

Rajamane NP, Nataraja MC, Lakshmanan N (2011) An introduction to geopolymer concrete. Indian Concr J 85:25–28

Rashad AM (2013) A comprehensive overview about the influence of different additives on the properties of alkali-activated slag - A guide for civil engineer. Constr Build Mater 47:29–55. https://doi.org/10.1016/j.conbuildmat.2013.04.011

Riahi S, Nazari A, Zaarei D et al (2012) Compressive strength of ash-based geopolymers at early ages designed by Taguchi method. Mater Des 37:443–449. https://doi.org/10.1016/j.matdes.2012.01.030

Rodier L, Bilba K, Onésippe C, Arsène MA (2017) Study of pozzolanic activity of bamboo stem ashes for use as partial replacement of cement. Mater Struct Constr 50:. https://doi.org/10.1617/s11527-016-0958-6

Roy RK (1990) A Primer on the Taguchi Method. Society of Manufacturing Engineers

Şahin S, Kocaman B, Örüng I, Memiş S (2006) Replacing cattle manure ash as cement into concrete. J Appl Sci 6:. https://doi.org/10.3923/jas.2006.2840.2842

Sanjayan JG, Nazari A, Pouraliakbar H (2015) FEA modelling of fracture toughness of steel fibre-reinforced geopolymer composites. Mater Des 76:215–222. https://doi.org/10.1016/j.matdes.2015.03.029

Sarkar M, Dana K (2021) Partial replacement of metakaolin with red ceramic waste in geopolymer. Ceram Int 47:3473–3483. https://doi.org/10.1016/j.ceramint.2020.09.191

Shoaei P, Musaeei HR, Mirlohi F, et al (2019) Waste ceramic powder-based geopolymer mortars: Effect of curing temperature and alkaline solution-to-binder ratio. Construction and Building Materials 227:116686. https://doi.org/10.1016/j.conbuildmat.2019.116686

Siyal AA, Azizli KA, Man Z, Ullah H (2016) Effects of Parameters on the setting time of fly ash based geopolymers using Taguchi method. Procedia Eng 148:302–307. https://doi.org/10.1016/j.proeng.2016.06.624

Sua-Iam G, Makul N (2013) Use of increasing amounts of bagasse ash waste to produce self-compacting concrete by adding limestone powder waste. J Clean Prod 57:308–319. https://doi.org/10.1016/j.jclepro.2013.06.009

Suhendro B (2014) Toward green concrete for better sustainable environment. Procedia Eng 95:305–320. https://doi.org/10.1016/j.proeng.2014.12.190

Suksiripattanapong C, Kua TA, Arulrajah A et al (2017) Strength and microstructure properties of spent coffee grounds stabilized with rice husk ash and slag geopolymers. Constr Build Mater 146:312–320. https://doi.org/10.1016/j.conbuildmat.2017.04.103

Tahwia (2017) Performance of ultra-high performance fiber reinforced concrete at high temperatures. Int J Eng Innov Technol 1–7

Temuujin J, Rickard W, Lee M, Van RA (2011) Preparation and thermal properties of fi re resistant metakaolin-based geopolymer-type coatings. J Non Cryst Solids 357:1399–1404. https://doi.org/10.1016/j.jnoncrysol.2010.09.063

Thomas BS, Kumar S, Arel HS (2017) Sustainable concrete containing palm oil fuel ash as a supplementary cementitious material – a review. Renew Sustain Energy Rev 80:550–561

Vald J, Rodrigue C, Giogetti J, et al (2021) Evaluation of performances of volcanic-ash-laterite based blended geopolymer concretes : mechanical properties and durability. 34:. https://doi.org/10.1016/j.jobe.2020.101935

Villaquirán-Caicedo MA, de Gutiérrez RM (2018) Synthesis of ceramic materials from ecofriendly geopolymer precursors. Mater Lett 230:300–304. https://doi.org/10.1016/j.matlet.2018.07.128

Yang T, Wu Q, Zhu H, Zhang Z (2017) Geopolymer with improved thermal stability by incorporating high-magnesium nickel slag. Constr Build Mater 155:475–484. https://doi.org/10.1016/j.conbuildmat.2017.08.081

Yaprak H, Memis S, Kaplan G (2017) Effect of ındustrial wastes as replacement of fine aggregate on properties of concrete. J Sci Eng Res 4:228–235

Yaprak H, Alnkaa A, Memis S, Kaplan G (2018a) The effects of steam curing time on the geopolymer mortar. In: International Congress on Engineering and Life Science, ICELIS. pp 13–16

Yaprak H, Memis S, Kaplan G, et al (2018b) Effects on compressive strenght of accelerated curing methods in alkali activated mortars. Int J Sci Technol Res 4:

Yaprak H, Alnkaa A, Memis S, Kaplan G (2019) Effects of different curing conditions on the properties of geopolymeric mortar. MOJ Civ Eng 5:45–50. https://doi.org/10.15406/mojce.2019.05.00148

Yasaswini K, Rao AV (2020) Materials today : proceedings behaviour of geopolymer concrete at elevated temperature. Mater Today Proc 33:239–244. https://doi.org/10.1016/j.matpr.2020.03.833

Yildizay H, Gören R, Yanik G (2014) Use ofalunite as a starting materia l of geopolymer. AKU J Sci Eng 14:219–224

Zareei SA, Ameri F, Shoaei P, Bahrami N (2019) Recycled ceramic waste high strength concrete containing wollastonite particles and micro-silica: A comprehensive experimental study. Constr Build Mater 201:11–32. https://doi.org/10.1016/j.conbuildmat.2018.12.161

Zawrah MF, Sawan SEA, Khattab RM, Abdel-shafi AA (2020) Effect of nano sand on the properties of metakaolin-based geopolymer : study on its low rate sintering. Constr Build Mater 246:118486. https://doi.org/10.1016/j.conbuildmat.2020.118486

Zhao R, Yuan Y, Cheng Z et al (2019) Freeze-thaw resistance of Class F fly ash-based geopolymer concrete. Constr Build Mater 222:474–483. https://doi.org/10.1016/j.conbuildmat.2019.06.166

Zhou S, Chen X (2012) Pozzolanic activity of feedlot biomass (cattle manure) ash. Constr Build Mater 28:493–498. https://doi.org/10.1016/j.conbuildmat.2011.09.003

Zhou S, Tang W, Xu P, Chen X (2015) Effect of cattle manure ash on strength, workability and water permeability of concrete. Constr Build Mater 84:121–127. https://doi.org/10.1016/j.conbuildmat.2015.03.062

Zhou W, Yan C, Duan P et al (2016) A comparative study of high- and low-Al2O3fly ash based-geopolymers: the role of mix proportion factors and curing temperature. Mater Des. https://doi.org/10.1016/j.matdes.2016.01.084

Zhu W, Rao XH, Liu Y, Yang EH (2018) Lightweight aerated metakaolin-based geopolymer incorporating municipal solid waste incineration bottom ash as gas-forming agent. J Clean Prod 177:775–781. https://doi.org/10.1016/j.jclepro.2017.12.267

Živica V, Palou MT, Križma M (2015) Geopolymer cements and their properties: a review. Build Res J 61:85–100. https://doi.org/10.2478/brj-2014-0007